Assessment of CMIP6 Multi-Model Projections Worldwide: Which Regions Are Getting Warmer and Are Going through a Drought in Africa and Morocco? What Changes from CMIP5 to CMIP6?

Ayat-Allah Bouramdane

sustainability

MDPI

Article

Assessment of CMIP6 Multi-Model Projections Worldwide: Which Regions Are Getting Warmer and Are Going through a Drought in Africa and Morocco? What Changes from CMIP5 to CMIP6?

Ayat-Allah Bouramdane

Higher School of Energy Engineering, International University of Rabat (IUR), Technopolis Rabat-Shore Rocade Rabat-Salé, Rabat 11103, Morocco; ayatallahbouramdane@gmail.com

Abstract: Although climate change is an inherently global issue, its impacts will not be felt equally across Earth's pressure belts and continental-scale regions. This study seeks to examine which areas are becoming warmer and experiencing drought, with a particular focus on Africa, in light of its low historical emissions but poor economic capacity for mitigation and adaptation to climate change, and Morocco, whose conditional goal, which will be achieved with foreign assistance, is rated as "almost sufficient" but is not yet in compliance with the Paris Agreement's goal. We also explore the consistency and sources of uncertainty in Coupled Model Intercomparison Project Phase 6 (CMIP6) models and analyze what changes from CMIP5—whose projections are based on the Representative Concentration Pathways (RCPs)—to Shared Socio-Economic Pathways (SSPs)-based scenarios for CMIP6. We find that strong forcing, with no additional climate policies, is projected to raise the mean annual temperature over Morocco for the long-term period by 6.25 °C. All CMIP6 models agree that warming (resp. drought) will be greater over land masses and poles (resp. tropical and coastal regions) than over oceans and equatorial regions (resp. high latitudes, equatorial, and monsoon zones), but less so on the intensity of changes.

Keywords: Africa; climate change; coupled model intercomparison project phases 5 and 6; Morocco; precipitation; representative concentration pathways; shared socio-economic pathways; temperature; world

Citation: Bouramdane, A.-A. Assessment of CMIP6 Multi-Model Projections Worldwide: Which Regions Are Getting Warmer and Are Going through a Drought in Africa and Morocco? What Changes from CMIP5 to CMIP6? *Sustainability* **2023**, *15*, 690. https://doi.org/10.3390/su15010690

Academic Editors: Adam Choryński and Dariusz Graczyk

Received: 15 November 2022
Revised: 24 December 2022
Accepted: 26 December 2022
Published: 30 December 2022

1. Introduction

1.1. Research Motivation and Background

Climate change is a field of science that has been studied for a long time. However, there are still a lot of things we do not understand, and some of the unanswered questions may have a significant impact on how well our lives turn out in the future. For instance, although people tend to use the terms "global warming" and "climate change" interchangeably, global warming is just one aspect of climate change.

In fact, "global warming" refers to the increase in global temperature that is mostly the result of excess heat in the climate system brought on by the addition of greenhouse gases (GHGs) to the atmosphere during the Industrial Era. The main human activities that contribute to these extra-anthropogenic emissions include the combustion of fossil fuels (i.e., coal, oil, and natural gas), deforestation, agriculture, and changes in land use. The fourth [1], fifth [2], and sixth [3] Assessment Reports (ARs) of the Intergovernmental Panel on Climate Change (IPCC) provided unequivocal proof of man-made global warming. The natural internal variability of the climate system and natural external forcings, such as variations in solar activity, volcanic activity, changes in Earth's orbit, etc., are thought to have a minor impact on global warming [4].

Climate change is defined as a significant change in average weather conditions, such as becoming warmer, wetter, or drier over several decades or longer. The difference between

climate change and natural weather variability is in the long-term tendency. Increases in global air and ocean temperatures, increasing sea levels, a decrease in snow and ice cover, and modifications in rainfall patterns are all effects of global warming. The most recent IPCC report [3] presents a troubling picture: climate change is already having an influence on every corner of the world. However, different parts of the world are affected differently by climate change. These regional changes are expected to have an impact on our natural world [5,6], our energy systems [7], our economy [8], as well as pose a number of social threats [9] if we fail to halve GHG emissions this decade [10]—e.g., by examining Photovoltaic (PV), wind, and Concentrated Solar Power (CSP) integration, without and with different capabilities of thermal energy storage [11] (Chapter 3) (SMRY. [12]), examining which dispatchable solar technology (i.e., CSP versus PV with different thermal and battery energy storage durations) reduces the use of conventional generators more in optimal mixes with different levels of renewable penetration and variability and how that impacts the benefits of spatio-temporal complementarity [11] (Chapter 4) (SMRY. [13,14]), and exploring which renewable technology is sensitive or resilient to climate change and how the latter affects the seasonal and annual patterns of electricity consumption [11] (Chapter 5)—and immediately scale-up adaptation [15,16]—e.g., by developing agrivoltaic systems [17,18] and water desalination projects [19,20].

With 1.37 billion people (17.4 percent of the world's population [21]) and an economy dependent on rain-fed agriculture, Africa, the second-largest continent on Earth, has the fastest population growth and is also among the regions most vulnerable to climate variability and change due to its low capacity to combat climate change [22,23].

African countries have several common characteristics, including topography, water scarcity, and long and hot summers. Morocco, a country located in Northwest Africa, has two main climate zones that regulate its climate: the southern interior regions, which are on the outskirts of the Sahara, and the northern Mediterranean coastline regions. Between the western regions, which are impacted by humidity coming from the Atlantic coast, and the eastern boundary, which is influenced by dry air, is a distinct transitional zone formed by the Atlas and Rif mountain ranges.

With its new Nationally Determined Contributions (NDCs) [24], submitted on 20 June 2021, Morocco demonstrated its commitment to the principles of the Paris Agreement by strengthening its pledges. Despite having low per capita emissions as a developing nation [25], Morocco is assuming its responsibility in the face of a global climate emergency. The new target includes an unconditional (resp. a conditional) emissions reduction of 18.3% (resp. 45%) below the Business-As-Usual (BAU) scenario by 2030, up from a 17% (resp. 42%) reduction in the previous NDC, excluding Land Use, Land Use Change, and Forestry (LULUCF). In comparison to other nations, Morocco's conditional goal, which will be achieved with foreign assistance, is rated as "almost sufficient", meaning that it is not yet in compliance with the Paris Agreement's 1.5 °C temperature limit, but might be with slight improvements [26].

Given the vulnerability of Africa and particularly Morocco to climate fluctuations—determined by the latitudinal extension, the geographical diversities, and the ocean opening—assessing how well high-resolution climate models can capture the climate in such intricate areas, understanding the worldwide and regional climate phenomena, their variability and change, and identifying hot spots and vulnerable communities are key to better managing the resources and to mitigating and adapting to global climate change [27].

To understand climate change that has occurred in the past, is occurring now, or will occur in the future due to natural and unforced variability or a change in Radiative Forcing (RF)—i.e., a measure of how much the energy balance of the Earth system has changed as a result of external disturbances; positive RF causes warming and negative RF causes cooling—the Coupled Model Intercomparison Project (CMIP) was designed to provide a global experimental protocol for investigating the output of coupled Atmosphere–Ocean General Climate Models (GCMs) to support model diagnosis, validation, documentation,

and data access. This also allows for the improvement of climate models by comparing a wide range of model simulations to observations and to each other to see where they agree and disagree on future changes using a common set of future greenhouse gas, aerosol, and other climate forcing concentrations. Climate data from CMIP Phase 3 (CMIP3) [28] were analyzed in the IPCC's fourth AR [1] based on the Special Report on Emissions Scenarios (SRES) [29]—four emission scenario families (A1, A2, B1, and B2) depending on the focus of future development (economic-A or environmental-B) and on its homogeneity (globalized-1 or with regional focus-2). CMIP Phase 5 (CMIP5) [30] served as the basis for the fifth AR, released in 2013 and 2014 [2,31], based on four long-term GHG concentration trajectories known as Representative Concentration Pathways (RCPs) [32,33]. The earth–atmosphere system accumulates energy and heats up more as a result of increased concentrations and higher RF values, leading to a significant rise in global temperature. The numbering denotes a specific amount of RF measured in watts per square meter attained by 2100 (i.e., 2.6, 4.5, 6.0, and 8.5 W/m^2 of change over the pre-industrial period), in order to discern the severity of climate forcing. The sixth AR, published in 2021 and 2022 [3], draws from CMIP6 [34], the most recent compilation of models produced by the global climate science community, based on Shared Socio-Economic Pathways (SSPs) [35,36]. In contrast to RCPs, SSPs are scenarios of projected global socio-economic developments up to 2100 that represent five different future societies with widely varying challenges to mitigation and adaptation to climate change. These trends are then used to develop scenarios of GHG emission trajectories using Integrated Assessment Models (IAMs) [37,38]. Indeed, the SSP scenario experiments can be broken down into two pathways: SSP and RCP. The three numerals that make up the experiment's name indicate the two paths. The SSP storyline for socio-economic mitigation and adaptation difficulties is represented by the first digit (SSP1 "Green and sustainable pathway", SSP2 "Middle of the road", SSP3 "regional rivalry", SSP4 "inequality", and SSP5 "Fossil-fueled development"). The experiment's second and third digits represent the RCP climate forcing (ex. SSP1-2.6, SSP2-4.5, and SSP5-8.5). Using comparable RF developments enables a direct comparison of CMIP5 and CMIP6 simulations.

1.2. Existing Research

Several recent studies have used CMIP6 multi-model ensembles to analyze drought and warming changes at global [39] as well as regional scales, such as in South Asia [40], the arid northwest China [41] and India [42], the United States, Central America and the Caribbean [43], the Amazon River Basin [44], and the Mediterranean and Sahara regions [45].

The comparison of projections from multiple CMIP5 and CMIP6 historical and scenario simulations to quantify the effects of the already changing climate in various regions of the world [46], including the Mediterranean region [47], the Middle East and North Africa (MENA) region [48], the Sahel [49], Bangladesh [50], Europe [51], and Australia [52], is still of substantial importance.

While these abovementioned studies have examined the improvement of the latest CMIP6 over CMIP5 for temperature and precipitation simulations, there are other published studies that focus only on CMIP5, particularly in Africa [53,54].

The assessment of climate change impacts in Morocco has been widely reported in the past [55,56]. Most studies in the field of climate change have only focused on CMIP3 [57] and CMIP5 scenarios [58]. Bouramdane et al. [11] (Chapter 5) examined the effects that projected climate change will have on the regional Moroccan mix by the end of the twenty-first century (2071–2100) in comparison to the historical period (1976–2005), compared this effect to the effect of the rental cost in the context of cost reduction of low carbon technologies, assuming a business-as-usual world in which nothing is done to combat climate change (RCP8.5), and highlighted the conditions for climate-resilient renewable mixes. Recent studies have examined how climate change affects the best locations for

solar photovoltaic and concentrated solar power plants [59], as well as offshore [60] and onshore [61] wind farms, using a multi-criteria decision-making framework.

1.3. Knowledge Gap

Even the impacts of climate change around the world have been widely assessed in the literature based on CMIP5 and CMIP6 projections. However, the complete picture is still unclear. First, these climate projections were assessed using different time periods and scenarios. Another critical point is the lack of a clear explanation for different climate signals in different pressure belts and continental-scale regions (for example, the land–ocean warming contrast, which parts of the planet are warming the fastest and why, are the Arctic and Antarctica experiencing the same thing, and why different rainfall patterns exist in tropical, desert, mid- and high-latitude areas). Second, despite the thorough projections that have been conducted in many regions of the world, there remain certain uncertainties and biases in the model results. Such model biases cast aspersions on the reliability of the estimates, thus requiring a concentrated effort for multi-model projections by assessing the level of consistency of the projections amongst the various climate models in different regions and discussing the sources of uncertainty. Third, there has been little discussion about the impacts of climate change on temperature and precipitation in Africa. While some studies have looked into the impacts of climate change, based on CMIP6, in southern West Africa [62] and over East Africa [63], the only study that investigates the whole continent was conducted by Almazroui et al. [64]. So far, however, no previous study has investigated the future warming and drought tendency in Morocco's sub-regions based on the latest iteration of CMIP6 climate scenarios (SSPs). In addition, despite the dire conclusions of several research works studying climate change impacts at various geographical scales and tracking pledges and current climate policies and progress towards the internationally agreed-upon goal of holding warming well below 2 °C, and pursuing measures to limit warming to 1.5 °C, there is still skepticism that the 2100 warming projections are alarmist, or at least overstated [65,66], particularly at the national scale. For instance, much uncertainty still exists about the relationship between Morocco's policies and warming projections. Fourth, the comparison of CMIP5 climate projections to the most recent generation of climate models developed for CMIP6 suffers from a lack of studies on Morocco.

1.4. Research Questions

This study seeks to fill this knowledge gap and provides a contribution in this direction by addressing the following research questions:

1. How do various places on the Earth (i.e., pressure belts and continental-scale regions) respond to forcing, considering the medium pathway of future GHG emissions with intermediate climate change mitigation and adaptation challenges?
2. Where do CMIP6 climate models provide a robust and unambiguous picture of significant climate warming and drought? What are the origins of systematic model biases?
3. How would a range of potential future scenarios of global GHGs affect temperature and rainfall in Africa's sub-regions? How fast is Morocco going to warm? Is it going to be 1 °C or more on average and with current trends before the end of the twenty-first century? How much warmer will Morocco's sub-regions become in the future? Which parts of Morocco will suffer from drought?
4. How does the CMIP6 model change the picture of CMIP5's climate projections over Africa and Morocco?

1.5. Methodology

To answer the abovementioned research questions and to provide guidance for climate policy at different temporal and spatial scales, we use the outputs of various GCMs provided by CMIP6 under three SSPs, referred to as SSP1-2.6, SSP2-4.5, and SSP5-8.5, respectively, for weak, moderate, and strong forcing. First, we consider the projections that cover the entire globe and examine the overall performance of seven GCMs in simulating

the temperature and precipitation under the medium pathway of future GHG emissions, SSP2-45, over both the past (from 1850 to 2014) and future (from 2015 to 2100) periods. Then, we compare the behavior of SSP2-4.5 and SSP5-8.5 CMIP6 climate scenarios to their CMIP5 predecessors—whose projections are based on the RCP scenarios—in representing the entire African continent and particularly the response of Morocco's sub-regions to climate change. The CMIP5 climate model has been used to run the climate experiments, including a simulation of the historical period (1971–2000) and a range of projections (2071–2100), RCP4.5 and RCP8.5, which explore ways in which the climate could evolve in the future. In Morocco, temperature changes based on CMIP6 are computed for three future time slices: 2010–2039 (near term), 2040–2069 (mid-term), and 2070–2099 (long term), all relative to the current climate (1980–2009). We also investigate whether the projected patterns of winter and summer temperature and rainfall for the twenty-first century exhibit spatial distributions that are similar to the yearly trends.

1.6. Originality of This Study and Implications

Governments are not the only parties tasked with reducing vulnerability and putting adaptation plans into action. Due to the severity of climate change, both public and private actors must collaborate to lessen susceptibility and adapt to the repercussions. Not all stakeholders, however, are aware of the vulnerable areas and the measures they can undertake to pro-actively prevent climate change and adapt to it. Projected changes in temperature and rainfall in climate-disaster-prone areas provide the essential foundation for climate change research studies and are vital for planning climate change mitigation and increasing our adaptation capacity to respond effectively.

This study has been one of the first attempts to thoroughly examine the impact of climate change at various geographical scales (the world, Africa, with a particular focus on Morocco, where agriculture [67] and water resources [68] are the most susceptible to these annual and seasonal projected changes), shedding light on the land–ocean warming contrast, the polar amplification, the sources of uncertainty in CMIP6 climate projections, and changes from RCP-based scenarios for CMIP5 and SSP-based scenarios for CMIP6.

1.7. Outline

This paper has been organized in the following way: After this introduction, which gives a brief overview of the research motivation, existing studies on climate change, knowledge gap, research questions of this study, a brief overview of the methodology adapted, the originality of this study, and implications, Section 2 introduces the study areas (Section 2.1) and the data computed in the framework of CMIP5 and CMIP6 (Section 2.2). Results are discussed next (Section 3). A summary and discussion of the projected changes in temperature and precipitation and further directions for impact assessments are provided in Section 4.

2. Methodology

In this part, we provide a brief overview of the study areas (Section 2.1) and the data computed in the framework of Phases 5 and 6 of the Coupled Model Intercomparison Project (Section 2.2).

2.1. Study Areas

To answer the first and second research questions of this study (mentioned in Section 1.4), we conducted an analysis over different pressure belts and six continental-scale regions, namely North America (NAM), Europe (EUR), Asia (AS), South America (SAM), Africa (AFR), and Australia (AUS), as shown in the top panel of Figure 1.

For the third and fourth research questions (mentioned in Section 1.4), in which we assess the impact of climate change on Africa and particularly Morocco due to their sensitivity to climate change and lack of the infrastructure resources needed to mitigate and adapt to it [22,23], we conducted a regional analysis over eight of Africa's sub-regions

(bottom-left panel of Figure 1): North Africa (NAF), the Sahara (SAH), West Africa (WAF), Central Africa (CAF), North East Africa (NEAF), Central East Africa (CEAF), South East Africa (SEAF), and South West Africa (SWAF). The detailed justification for choosing these sub-regions is provided by Iturbide et al. [69].

The bottom-right panel of Figure 1 shows the four Moroccan regions considered in this study. Indeed, Morocco is located in the northwest corner of the African continent. Morocco's climate varies according to its topography, which ranges from the Mediterranean Sea and the Atlantic Ocean to the NORTH and WEST, respectively, to large Atlas mountainous areas in the CENTER, and the Sahara to the south EAST, and far SOUTH.

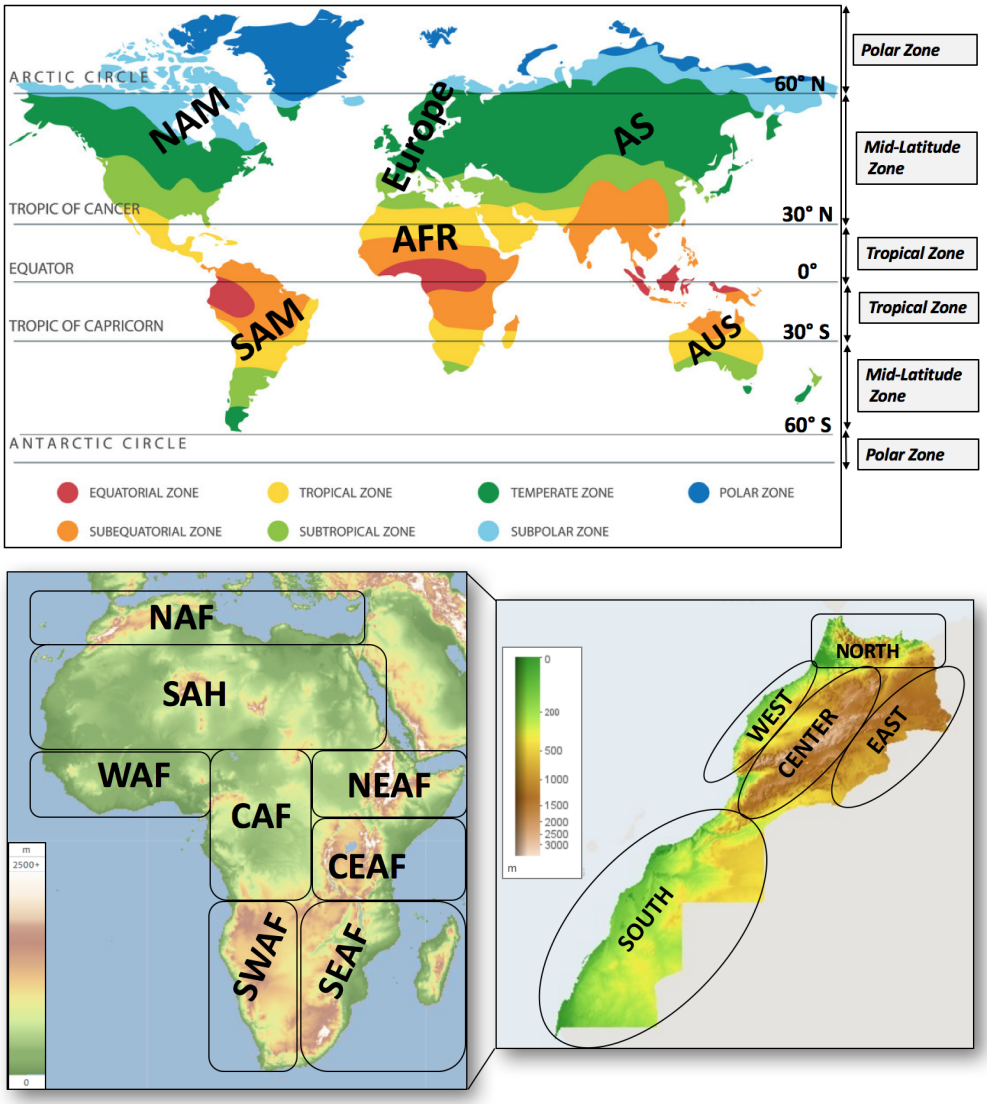

Figure 1. Top: Map displaying the Earth's pressure belts and six continental-scale regions: North America (NAM), Europe (EUR), Asia (AS), South America (SAM), Africa (AFR), and Australia (AUS). **Bottom:** Elevation (i.e., the height above the mean sea level) in (m) over: **Bottom-Left:** the eight sub-regions of Africa: North Africa (NAF), Sahara (SAH), West Africa (WAF), Central Africa (CAF), North East Africa (NEAF), Central East Africa (CEAF), South East Africa (SEAF), and South West Africa (SWAF). Source: own elaboration, adapted from the Global Wind Atlas [70] and Iturbide et al. [69]. **Bottom-Right:** the four Moroccan regions are: NORTH, EAST, WEST, and SOUTH. Source: own elaboration, adapted from the Moroccan Agency for Sustainable Energy's (MASEN) Solar Atlas [71].

2.2. CMIP5/6 Multi-Model Projections

Scientists use climate models to investigate how the climate has changed in the past, how it is changing now, and how it will change in the future by numerically solving partial differential equations representing physical, chemical, and biological processes and interactions on the Earth. Therefore, they represent a crucial tool for understanding the complexities of Earth's climate and are continually becoming more detailed and accurate. In fact, higher spatial resolution (i.e., by dividing the Earth into a series of boxes or "grid cells" and using "parametrizations" to represent processes that occur on scales smaller than the grid cells) and smaller time steps allow the model to produce comprehensive climate information for a specific area, but this comes at the expense of taking longer to run because the model must do more calculations in each run, which requires supercomputers with high computing power [72].

Whereas weather forecasting makes predictions of the conditions of the atmosphere over specific areas and over a short period of time, climate models are broader and analyze the long-term regional or global average of weather patterns over seasons, years, or decades.

In this study, we compute the changes in near-surface air temperature "tas" in Kelvin—the temperature of air at two meters above the surface of land, sea, or inland waters—and the mean precipitation flux "pr" which represents the amount of water per unit area and time (Kg· m^{-2}·s^{-1})—the total amount of rain and snow (both liquid and frozen water) that falls to the Earth's surface. It is the total of both convective and large-scale precipitation. It excludes fog, dew, and precipitation that evaporates in the atmosphere prior to reaching the Earth's surface from the CMIP6 [34] global climate projections and the COordinated Regional climate Downscaling EXperiment (CORDEX)-CMIP5 [30] regional climate projections available in the Climate Data Store (CDS) of the Copernicus Climate Change Service (C3S) [73].

For both CMIP6 and CMIP5, the projected temperature change (°C) is calculated as the difference between the projected horizon mean and the baseline mean. This "delta approach" takes the climate change signal as the difference between the future and the past. Precipitation changes are calculated as the Relative Change "RC" (%) between the projection and baseline periods using the following formula: RC = (projection – baseline)/baseline.

2.2.1. CMIP6 Global Climate Projections

CMIP6 global climate projections are based on climate system simulations performed with General Circulation Models (GCMs), which describe physical processes in the atmosphere, ocean, cryosphere, and land surface. These "coupled" Atmosphere–Ocean GCMs (AOGCMs) models cover the entire globe and use information about the system's external impacts.

CMIP6 climate projections provide daily and monthly global climate projections data from a wide range of experiments, climate models, and time periods.

The term "experiments" refers to the:

- **Historical experiment**, performed with a coupled AOGCM, covering the period where modern climate observations exist (1850–2014). The model is forced by changing conditions, which include atmospheric composition, land use, and solar forcing (consistent with observations). The pre-industrial control simulation is used to generate the initial conditions. The historical simulation is used to compare model performance to observed climate change and can be used as a reference period for future scenario runs.
- **Future scenarios experiment**, performed also with a coupled AOGCM, and covering the period 2015–2100, following the Shared Socio-Economic Pathway (SSP) and Representative Concentration Pathway (RCP) combination pathways. The SSP scenarios describe multiple pathways of future climate forcing that encompass a wide range of conceivable social and climatic futures, from best-estimated warming of less than 1.5 °C to more than 4 °C warming by 2100. The scenarios are, in fact, the outcome of sophisticated calculations that are dependent on how quickly humans

reduce greenhouse gas emissions. However, the computations are also intended to account for socio-economic changes such as population, education, land use, and so on. For instance, an increase in population is expected to increase demand for fossil fuels and water. Education can influence the rate at which technology advances. Emissions rise when forest area is converted to agricultural land. Each scenario is labeled to identify both the emissions level and the so-called SSP, which is employed in those computations [74]. Figure 2 illustrates how the different SSPs differ in terms of socio-economic characteristics (top panel) and hence mitigation and adaptation challenges (bottom panel). For example, experiment:

- **SSP1 "Green Road"** describes an increasingly sustainable world where global commons are preserved, the limits of nature are respected, the focus is more on human well-being than on economic growth, investments in education and health go up, income inequalities between and within states are being reduced, and consumption is oriented towards minimizing material resource and energy usage [75]. As a result, the challenges to mitigation and adaptation are relatively low (bottom panel of Figure 2).
- **SSP2 "Middle of the Road"** defines a world in which social, economic, and technological trends do not deviate significantly from historical and existing patterns. Development and income growth vary dramatically, with some countries making relatively excellent progress while others lag. There is some cooperation among states, but progress toward reaching sustainable development goals is modest. Environmental systems deteriorate, despite some improvements, and the intensity of resource and energy use decreases overall. Global population growth is moderate, leveling off in the second half of the century. Income inequality remains or improves slowly, and challenges to minimizing susceptibility to societal and environmental changes persist [76]. With these moderate development patterns, the world faces moderate mitigation and adaptation challenges (bottom panel of Figure 2), but with significant heterogeneity across and within countries.
- **SSP3 "Regional Rivalry"** describes a scenario in which the resurgence of nationalism and regional conflicts push global issues to the margins. Policies are increasingly focusing on national and regional security concerns. Countries prioritize fulfilling energy and food security goals within their own regions over broad-based development. Inequality is increasing, and certain regions are suffering from severe environmental harm. Investments in education and technological development are declining. Population growth is modest in developed countries and high in developing countries. Economic progress is gradual, and material-intensive consumption persists or worsens over time. A low worldwide priority for resolving environmental problems leads to severe environmental degradation in some locations [77]. Mitigation will be difficult due to increasing resource intensity and reliance on fossil fuels, as well as difficulties in achieving international collaboration and delayed technological advancement (bottom panel of Figure 2). The limited progress on human development, poor income growth, and lack of effective institutions, particularly those that can act across regions, imply high adaptation challenges for many groups across all regions (bottom panel of Figure 2).
- **SSP4 "Inequality"** is a scenario in which the gap between internationally collaborating developed nations and those stuck at a lower developmental stage with poor income and education is expanding. High differences in human capital investment, combined with growing disparities in economic opportunities and political power, contribute to increased inequalities and stratification both between and within countries. Social cohesion deteriorates, and conflict and instability become more widespread. The high-tech economy and sectors are seeing rapid technological growth. The global energy market is diversifying, with investments in both carbon-intensive fuels such as coal and unconventional oil

as well as low-carbon energy options. Environmental strategies are focused on local challenges in moderate- and high-income communities [78]. This results in low mitigation and high adaptation challenges (bottom panel of Figure 2). If we continue on this path, average temperatures will rise by 3.6 °C.

– **SSP5 "Fossil-Fueled Development"** is a scenario in which global markets become more integrated, resulting in innovations and technological advancement. The global economy is expanding, while local environmental issues such as air pollution are being successfully addressed [79]. In addition, there are significant investments in health, education, and institutions to improve human and social capital. However, global social and economic development is based on increased exploitation of fossil fuel resources, particularly coal, and an energy-intensive lifestyle, which results in potentially high mitigation challenges (bottom panel of Figure 2). While technological solutions efficiently handle local environmental problems, there is very little effort to avoid future global environmental impacts due to a perceived trade-off with economic growth. Human development goals, strong economic growth, and highly engineered infrastructure result in relatively minor adaptation challenges for all (bottom panel of Figure 2).

The Intergovernmental Panel on Climate Change (IPCC) Sixth Assessment Report (AR6) [3] assessed the projected temperature outcomes of a set of five scenarios based on the framework of the SSPs: SSP1-1.9 (a new pathway in 2100 that uses a relatively low radiative forcing of 1.9 W/m^2 to model how people can keep warming below the 1.5 °C threshold), SSP1-2.6, SSP2-4.5, SSP3-7.0 (which indicates a forcing level between RCP6.0 and RCP8.5, covers a gap in the CMIP5 forcing pathways), and SSP5-8.5 [74,80]. The name of these scenarios consists of the SSP on which they are based, combined with the expected level of radiative forcing (RF) in the year 2100 (1.9 to 8.5 W/m^2). In this study, three SSPs have been used:

- **SSP1-2.6** is based on SSP1, which has minimal climate change mitigation and adaptation issues, and RCP2.6, a future pathway with an RF of 2.6 W/m^2 in the year 2100. The SSP1-2.6 scenario illustrates the low end of potential future forcing paths and the most optimistic scenario, in which global CO_2 emissions are reduced to zero by 2050. It is the only one that satisfies the Paris Agreement's aim of restricting global warming to roughly 1.5 °C over pre-industrial levels, with warming peaking at 1.5 °C but then declining and stabilizing at 1.4 °C by the end of the century.
- **SSP2-4.5** is a scenario that follows SSP2, a storyline with intermediate mitigation and adaptation issues, and RCP4.5, which leads to an RF of 4.5 W/m^2 by the year 2100. The SSP2-4.5 scenario indicates the medium portion of probable future forcing routes. This scenario is roughly in line with the Paris Agreement's pledges and ambitions. The scenario deviates slightly from the "no-extra climate policy" reference scenario, resulting in a best-estimated warming of around 2.7 °C by the end of the twenty-first century.
- **SSP5-8.5** is based on SSP5, in which climate change mitigation issues dominate but with low adaptation challenges, and RCP8.5, a future pathway with an RF of 8.5 W/m^2 in the year 2100. The SSP5-8.5 scenario represents the most likely future forcing pathways in the absence of additional climate policies. It can be understood as an update of the CMIP5 scenario RCP8.5, now combined with socio-economic considerations. By 2100, the average global temperature will be 4 °C higher.

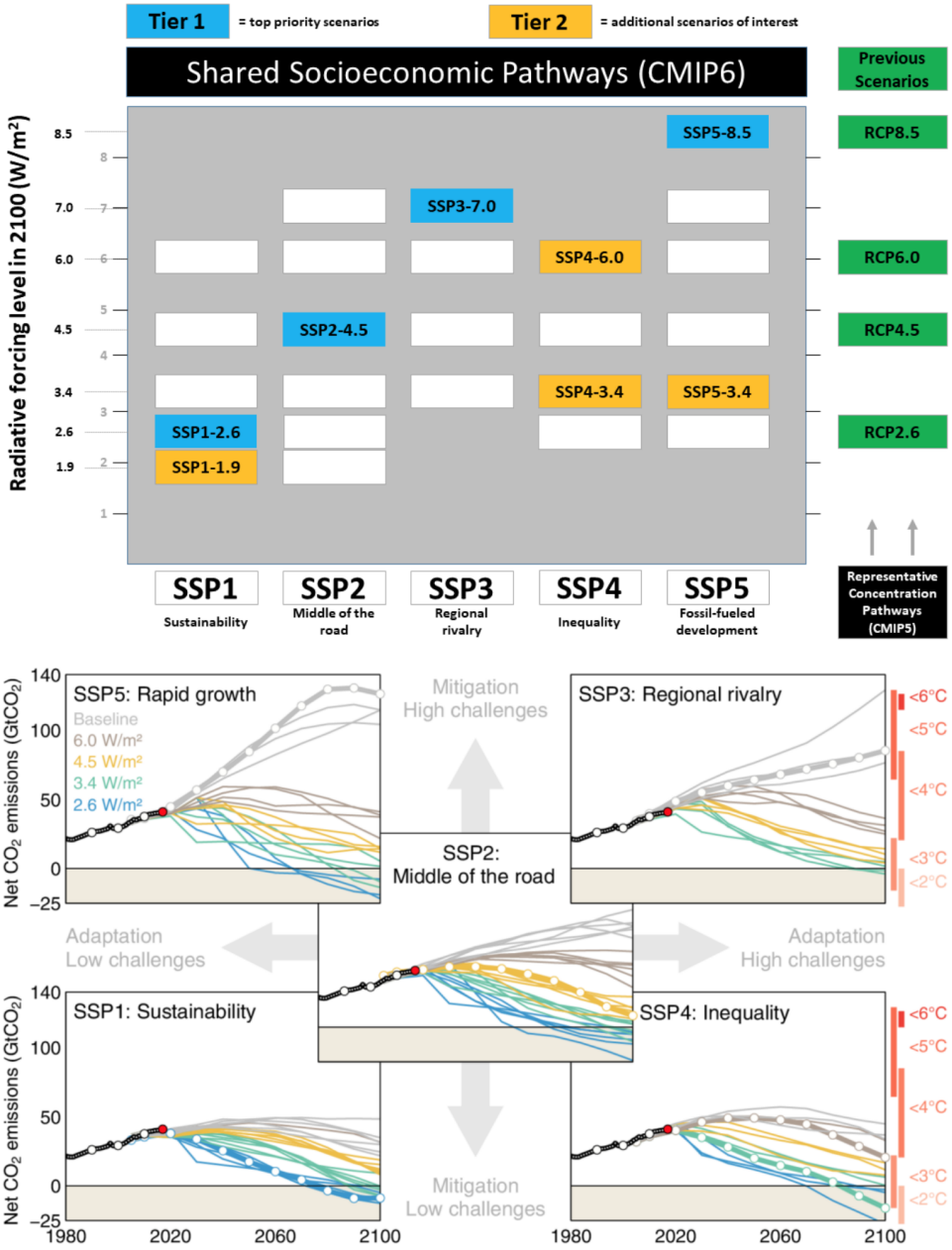

Figure 2. Top: A matrix depicting all possible Shared Socio-Economic Pathways (SSPs)-based scenarios for Coupled Model Intercomparison Project Phase 6 (CMIP6) in the abscissa and radiative forcing (RF) combinations in the ordinate. The color-coding is to indicate the priority of each scenario. Tier 1 in blue, or top priority scenarios, are SSP1-2.6, SSP2-4.5, SSP3-7.0, and SSP5-8.5. Three of the four Tier 1 scenarios are updated versions of prior CMIP5 Representative Concentration Pathway (RCP) scenarios depicted in green (RCP2.6, RCP4.5, and RCP8.5) to enable easy comparison between CMIP5 and CMIP6 projections. Tier 2 scenarios, in yellow, are SSP1-1.9, SSP4-6.0, SSP4-3.4, and SSP5-3.4. They are either not viable or have not been prioritized by the Scenario Model Intercomparison Project (ScenarioMIP) [35]. Individual scenarios are denoted by the name of the fundamental pathway, followed by two numerals indicating the increased RF achieved by the year 2100 in W/m^2 units. **Bottom:** SSP and their associated challenges of adaptation (in abscissa) and mitigation (in ordinate) to climate change. A rapid transition to zero or negative emissions is critical in pathways consistent with the 1.5–2 °C target. Chart from the Global Carbon Project [81].

The CMIP6 climate models obtained from CDS are detailed in Table 1, including the name of the modeling center and where information is readily available.

Table 1. CMIP6 climate models used to project future climate change impacts on temperature and rainfall, with their name and country **(first column)** as well as the modeling center **(second column)**. The interested reader is referred to the sources indicated for a full description of the climate models **(third column)**. Source: Own elaboration, additional information about the CMIP6 models can be found in [82,83].

Seven CMIP6 Global Climate Models		
Model Name	**Modeling Center**	**Key Reference**
HadGEM3-GC31-LL	Met Office Hadley Centre, Natural Environmental Research Council (MOHC-NERC)	Ridley et al. (2018) [84].
INM-CM4-8 (Russia)	Institute of Numerical Mathematics (INM)	Volodin et al. (2018) [85].
INM-CM5-0 (Russia)	Institute of Numerical Mathematics (INM)	Volodin et al. (2022) [86].
IPSL-CM6A-LR (France)	Institut Pierre-Simon Laplace (IPSL)	Boucher et al. (2020) [87].
MIROC-ES2L (Japan)	Atmosphere and Ocean Research Institute (AORI) and Centre for Climate System Research—National Institute for Environmental Studies (CCSR-NIES)	Hajima et al. (2019) [88].
MPI-ESM1-2-LR (Germany)	Max Planck Institute for Meteorology (MPI-M), Alfred Wegener Institute (AWI) "MPI-M AWI"	Mauritsen et al. (2019) [89].
UKESM1-0-LL (United Kingdom)	Met Office Hadley Centre (MOHC), Natural Environmental Research Council (NERC), National Institute of Meteorological Science—Korean Meteorological Administration (NIMS-KMA), National Institute of Weather and Atmospheric Research (NIWA)	Sellar et al. (2019) [90].

The preparation steps to examine the changes in temperature and precipitation include temporal aggregation (i.e., aggregate over time) and spatial aggregation (i.e., average over latitude and longitude dimensions) to have a single monthly or annual and global or regional value for each climate model, experiment, and time horizon. A very important consideration, however, is that gridded data cells do not all correspond to the same areas. In fact, because the Earth is a sphere, the area covered by each climate data point varies as a function of latitude (i.e., smaller at the poles and larger at the equator). We need to take this into account when averaging. One way to do this is to use the cosine of the latitude as a proxy for the varying sizes. This can be implemented by first calculating weights as a function of the cosine of the latitude, then applying these weights to the data. The next step is to compute the mean across the latitude and longitude dimensions of the weighted data.

2.2.2. CORDEX-CMIP5 over Africa: Regional Climate Projections

Due to their coarse spatial resolution, GCMs can resolve only the larger scales of atmospheric circulation. They provide important information on global to sub-continental scales of climate change. They cannot, however, capture the effects of local forcing (e.g., complicated terrain, coasts, and land cover), which alters the climate signal [91]. Regional Climate Models (RCMs), on the other hand, generate climate information in greater detail for a specific area and in a reasonable time by taking initial and lateral boundary conditions

from GCMs or reanalysis. This is called "dynamical downscaling". Several international projects are developing RCMs to dynamically downscale GCM data with the purpose of delivering local high-resolution climate data [91,92]. The North American Regional Climate Change Assessment Program (NARCCAP) [93] supplied simulations for the North American continent, and PRUDENCE [94] and ENSEMBLES [95] provided simulations for the European areas. The COordinated Regional climate Downscaling EXperiment (CORDEX) [91] is a World Climate Research Program (WCRP) supported to generate regional climate change scenarios for fourteen regions that cover the majority of the world's geographical areas. The EURO-CORDEX [96] and MED-CORDEX [97] provide regional climate projections for Europe and the Mediterranean region, respectively, as part of the global CORDEX framework. Another method of downscaling is called "statistical downscaling", which involves using observed data to derive a statistical relationship between the global and local climates (for additional information, see (Chapter 2, Page 60) [11]).

In this study, we use CORDEX-CMIP5 regional climate data with a spatial resolution of $0.44 \times 0.44^{\circ}$ (Africa's domain) to make climate projections over Africa and Morocco. We use data from the RCM "CanRCM4" with lateral boundary conditions from the GCM "CanESM2", both from the Canadian Centre for Climate Modeling and Analysis. This coupled model is referred to as "CanRCM4–CanESM2". Bouramdane et al. (Chapter 5 [11]), who assess the consistency of CMIP5 climate projections by running two RCM simulations (the version 4 of the Rossby Centre regional Atmospheric model "RCA4" and the version 351 of the Weather Research and Forecasting model "WRF351") with boundary conditions from four different GCMs (the Centre National de Recherches Météorologiques-Coupled Model "CNRM-CM5", the Earth System Model "EC-EARTH", the Geophysical Fluid Dynamics Laboratory's Earth System Model "GFDL-ESM2M", and the Community Climate System Model "CCSM4"), show that the GCM has a minor impact on the robustness of climate projections when compared to the GCM + RCM-induced spread. In fact, the results are sensitive to RCM uncertainty because major differences in the mean and variance of projections across the four CORDEX-CMIP5 models are more visible when the RCM is changed. Therefore, in this study, for sake of simplicity, we use one specific CMIP5 model (to be compared to the CMIP6 HadGEM3-GC31-LL climate model). We consider historical (covering the period 1971–2000) and future scenarios experiments (covering the period 2071–2100), which provide different pathways of future climate forcing: RCP4.5 (i.e., medium-low emissions scenario) and RCP8.5 (i.e., high-end emissions or "business as usual" scenario). RCP2.6 (i.e., a stringent mitigation scenario) and RCP6.0 (i.e., a medium-high emission scenario) are not used in this study.

3. Results

In this section, we aim to answer the research questions raised in Section 1.4 from a more detailed perspective. First, we start by examining how the temperature in various places on the Earth responds to forcing and how precipitation patterns are changing as a result of the SSP2-4.5 global climate change scenario (Section 3.1). Second, we explore the level of consistency in the CMIP6 climate projections amongst the seven climate models on the response of the worldwide temperature and precipitation to this "middle of the road" scenario (Section 3.2). Third, we analyze how a range of potential future scenarios of global greenhouse gases (GHGs) affect the temperature and rainfall in different parts of Africa (Section 3.3.1), and particularly how much warmer Morocco will become in the future and which parts of Morocco will suffer from drought (Section 3.3.2). Finally, we examine what changes from CMIP5—whose projections are based on medium-low and high-end emission scenarios (RCP 4.5 and RCP 8.5)—to SSP-based scenarios for CMIP6 (Section 3.4).

3.1. Worldwide CMIP6 Climate Projections

This section aims to answer the first research question of this study (Section 1.4). To do so, we examine the projected mean changes in temperature (top panel of Figure 3) and precipitation (bottom panel of Figure 3), across the world (top panel of Figure 1), considering

the CMIP6 HadGEM3-GC31-LL climate model (Table 1), under the medium pathway of future GHG emissions with intermediate climate change mitigation and adaptation challenges "SSP2-4.5" (bottom panel of Figure 2), over one time horizon (2015–2100) relative to the historical period (1850–2014). In fact, we use the historical experiment to compute the past climatology and repeat the step to compute the projected climatology according to the SSP2-4.5 scenario. Finally, we take the difference between the two in order to assess the extent of change.

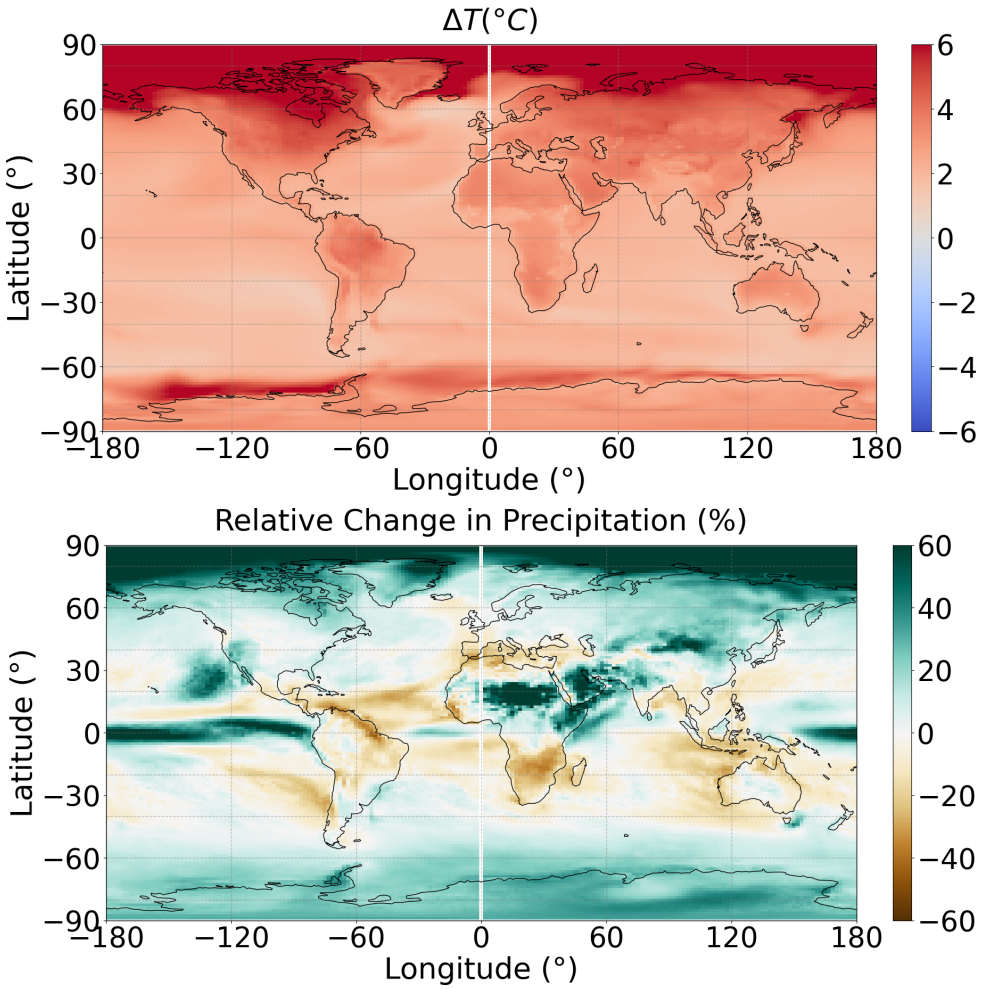

Figure 3. CMIP6 projection of the change in near-surface temperature (°C) (**top**) and the relative change (%) in precipitation (**bottom**) climatology by the end of this century (2015–2100) relative to the historical reference forcing (1850–2014), across the world (top panel of Figure 1), with the longitude (°), in abscissa, and the latitude (°), in ordinate. Data from the HadGEM3-GC31-LL climate model (Table 1), under the medium emissions Shared Socio-Economic Pathway (SSP) "SSP2-4.5" (Section 2.2.1, Figure 2). The color intensity on the color bar depicts the variation over time, with temperature (resp. precipitation) increasing in red (resp. green) and decreasing in blue (resp. brown). Source: Own elaboration.

3.1.1. Exceptional Warmth in Some Regions

While the average global temperature is rising, the rate of warming is not uniform around the globe, as illustrated in the top panel of Figure 3.

A few insights can be drawn from the top panel of Figure 3. First, the continents are expected to warm more than coastal areas (see discussion in Section 4.4). Second, the temperatures are warming faster at high latitudes, especially in and near the Arctic, than places close to the equator (see discussion in Section 4.5). However, it does not concern the Arctic and Antarctica in the same way (see discussion in Section 4.6).

3.1.2. Precipitation Patterns

The bottom panel of Figure 3 shows the projected percentage change (%) in precipitation by the end of the 21st century (2015–2100) relative to the historical period (1850–2014) under the SSP2-4.5 climate change pathway. Green color shows areas where precipitation is expected to increase, while brown areas indicate less future rain and snow. The hatching shows areas with low model agreement.

As can be seen in the bottom panel of Figure 3, precipitation is expected to increase in many places on the planet in the future. The regional heterogeneity of the rise in precipitation magnitude is, however, significant (see discussion in Section 4.7). We note that the equatorial regions and some areas in the tropics receive increased precipitation (see discussion in Section 4.8). Furthermore, due to sinking, dry air from high pressure systems, desert areas (mostly between 15° and 35° north and south of the equator) receive little rainfall (bottom panel of Figure 3) (see discussion in Section 4.9). The presence of semi-permanent subtropical anticyclones causes the air to subside and become warm and dry in the subtropics (top and bottom panels of Figure 3). The Mediterranean region is particularly vulnerable to climate change, as it is expected to have around 5–35 percent less precipitation by 2100 in a SSP2-4.5 scenario. Together with the amplified Mediterranean drought, precipitation decreases have been observed in southern Africa, western Australia, Chile, and Central America/Mexico (bottom panel of Figure 3).

The HadGEM3-GC31-LL climate model shows that the majority of the precipitation increase is projected to occur at high latitudes (bottom panel of Figure 3), particularly in the Arctic, where warmer oceans increase the amount of water that evaporates into the air. Mid-latitudes are projected to receive a moderate amount of precipitation (bottom panel of Figure 3) (For more information, see Section 4.10).

3.2. Consistency of CMIP6 Climate Projections

This section aims to answer the second research question of this study (Section 1.4), in which we examine the regions where CMIP6 climate models provide a robust and unambiguous picture of significant climate warming and drought and the origins of systematic model biases.

Each global climate model of the seven CMIP6 climate models (Table 1) was evaluated independently according to its capacity to mimic the expected world's change in temperature climatology (°C) (Figure 4) and the world's relative change in precipitation (%) (Figure 5), between the past (1850–2014) and the future period including the end of the 21st century (2015–2100) under the SSP2-4.5 emission scenario. We consider that the multi-models considered in this study agree if all climate models (from Russia, France, Japan, Germany, and the United Kingdom) have the same sign of change (positive or negative) and provide coherent future projections.

While the CMIP6 climate models are confident in their projections of how different continental-scale regions will warm or cool or become wetter or drier, it should be noted that the seven climate models disagree on the magnitude of the projected temperature and precipitation changes (Figures 3–5).

3.2.1. Temperature Consistency

Temperature projections (top panel of Figure 3 and all panels of Figure 4) demonstrate a shift toward warmer conditions in all climate model simulations. As a result, these changes can be considered robust. As can be seen, there is widespread agreement among the models that coastal areas will have moderate temperature increases compared to land areas. The models also agree that both the Arctic and Antarctica will experience more warming in the future, but Antarctica will experience less temperature rise than the Arctic (as stated in Section 3.1.1).

Nevertheless, climate models are not reproducing the same projections in some areas (such as some areas in the North Pole in the INM-CM4-8, the MPI-ESM1-2-LR models,

and the South Pole in the MIROC-ES2L model, Figure 4a,e,d, which are projected to become cooler).

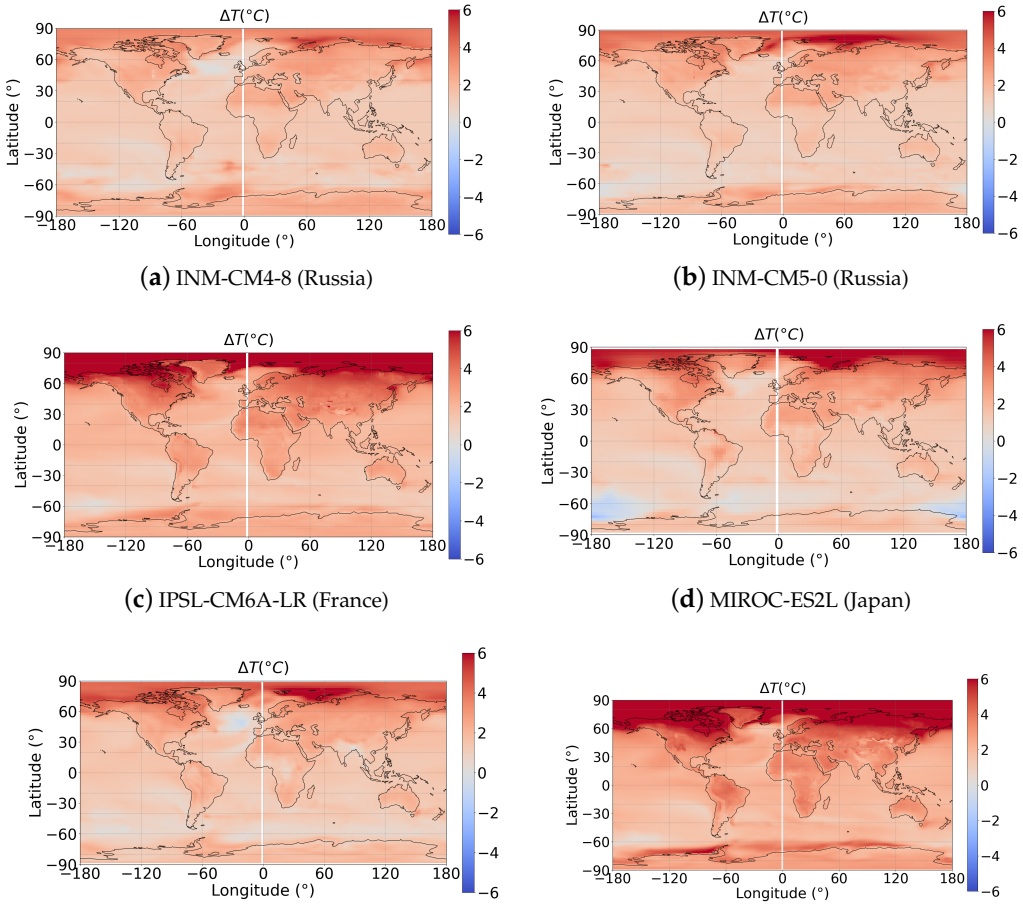

(**a**) INM-CM4-8 (Russia) (**b**) INM-CM5-0 (Russia)

(**c**) IPSL-CM6A-LR (France) (**d**) MIROC-ES2L (Japan)

(**e**) MPI-ESM1-2-LR (Germany) (**f**) UKESM1-0-LL (United Kingdom)

Figure 4. Similar to Figure 3, but for only the change in near-surface temperature (°C) climatology. Instead of using the HadGEM3-GC31-LL climate model, climate data is computed from different climate models from different countries: (**a**) INM-CM4-8; (**b**) INM-CM5-0; (**c**) IPSL-CM6A-LR; (**d**) MIROC-ES2L; (**e**) MPI-ESM1-2-LR; (**f**) UKESM1-0-LL; see Table 1 to examine differences between CMIP6 climate models in simulating the climate change signal, as well as to capture the sources of uncertainty in future climate projections. As for the climatic mean, the results reveal close similarity between the CMIP6 models (i.e., robust signals of enhanced warming), but less so on the intensity of changes, and no climate model is clearly outperforming the others. Source: Own elaboration.

3.2.2. Precipitation Consistency

The bottom panel of Figure 3 and all panels of Figure 5 show the expected percent change in precipitation, with green areas indicating increased precipitation and brown areas indicating reductions. The hatching in the panels indicates areas where climate models do not agree on the direction of change.

CMIP6 climate models are confident that relatively wet areas, such as the tropics and high latitudes, will become wetter, while relatively dry areas, such as the subtropics (where most of the world's deserts are located), will become drier (see Section 3.1.2 for more information).

However, while some models (INM-CM4-8, INM-CM5-0, and MIROC-ES2L) show a slight increase or decrease in precipitation over most of the areas (Figure 5a,b,d), others (IPSL-CM6A-LR, MPI-ESM1-2-LR, and UKESM1-0-LL) show much greater changes (Figure 5c,e,f). For instance, the Russian and Japanese models project precipitation de-

creases of around 5–20% on average by the end of this century in the tropics. However, the French, German, and UK models project a 20–60% average decrease in precipitation by 2100. Sizable differences between dry and wet conditions can be found in many regions of the world.

Interestingly, despite all the focus on drought in Africa [23], CMIP6 climate models do not generally agree that a warmer globe will result in less rainfall across the entire continent (bottom panel of Figure 3, all panels of Figure 5 and Section 3.3.1).

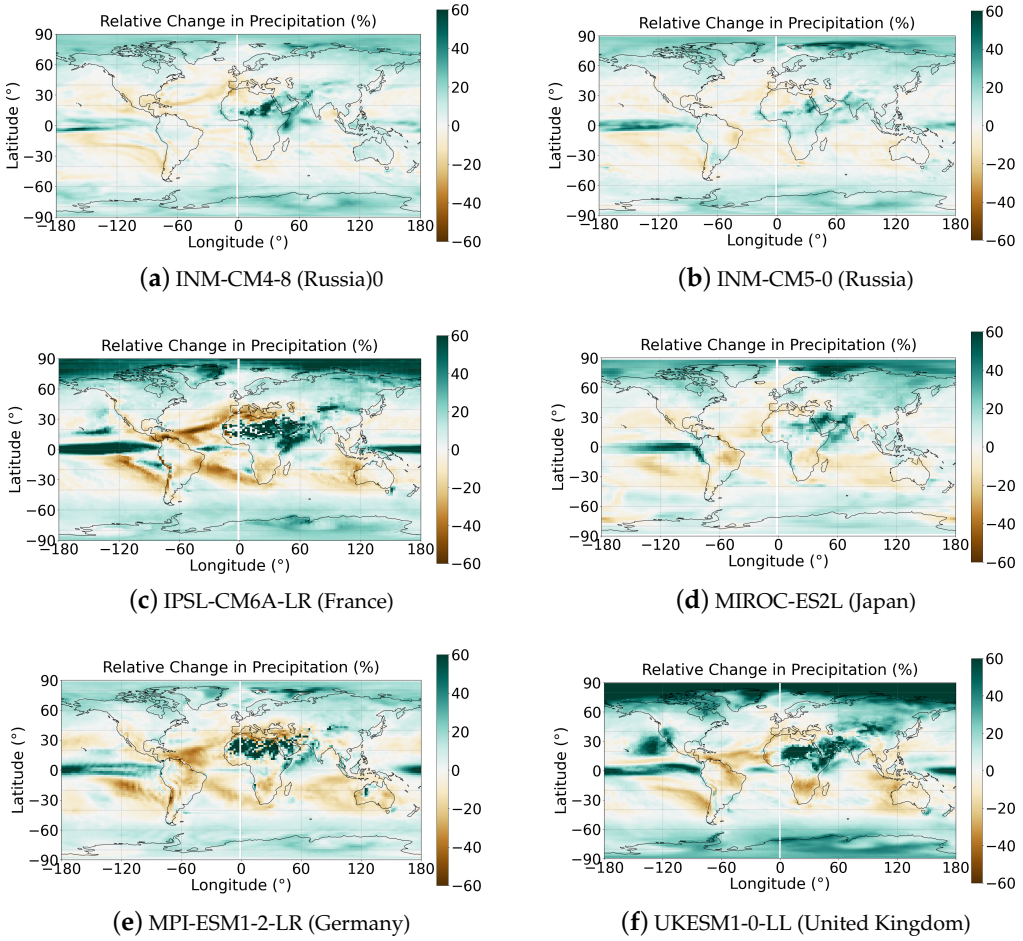

(**a**) INM-CM4-8 (Russia)0 (**b**) INM-CM5-0 (Russia)

(**c**) IPSL-CM6A-LR (France) (**d**) MIROC-ES2L (Japan)

(**e**) MPI-ESM1-2-LR (Germany) (**f**) UKESM1-0-LL (United Kingdom)

Figure 5. Similar to Figure 4, but for the relative change (%) in precipitation. Source: Own elaboration.

More discussion on the sources of uncertainty associated with future projections, including the reasons for the inconsistencies in the results generated based on different models, can be found in Section 4.11.

3.3. Potential Climate Change Impacts over Africa and Morocco: Intercomparison of SSP Scenarios

This section aims to address the third research question of this study (Section 1.4), which explores how hot Africa (Section 3.3.1), and in particular Morocco (Section 3.3.2), will become by 2100, taking into account various levels of political efforts to slow down and adapt to climate change.

3.3.1. Africa'S CMIP6 Climate Projections

We examine future changes in temperature (°C) (left panels of Figure 6) and precipitation (%) (right panels of Figure 6), in the twenty-first century (2015–2100) against the reference climate (1985–2014), over Africa's eight sub-regions defined in the bottom-left panel of Figure 1, using data from the HadGEM3-GC31-LL climate model (Table 1), under

three future Shared Socio-Economic Pathways (SSPs), namely: a low (SSP1-2.6), medium (SSP2-4.5), and strong forcing scenario (SSP5-8.5) (Section 2.2.1, Figure 2).

Overall, the agreement between CMIP6 climate models on the signs of change is extremely high (see Africa's projections in Figures 4 and 5).

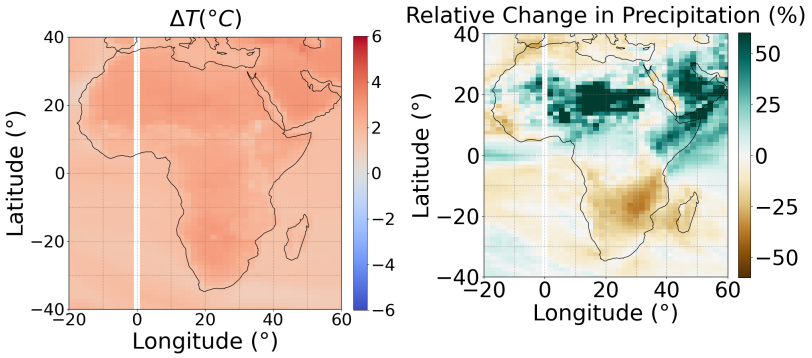

(**a**)

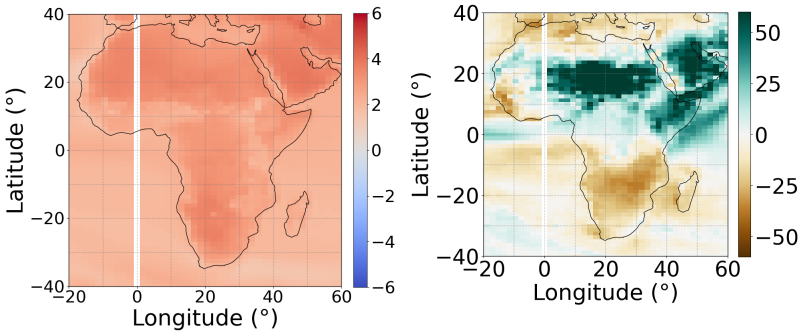

(**b**)

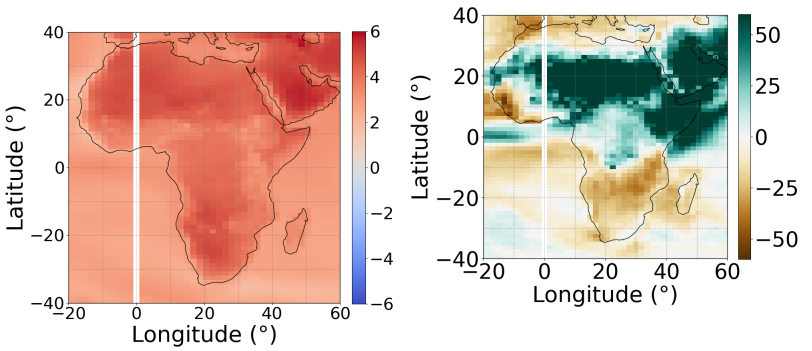

(**c**)

Figure 6. Similar to Figure 3, but numerical simulations are performed across Africa's eight sub-regions (bottom-left panel of Figure 1), under three future Shared Socio-Economic Pathways (SSPs): high (**top**), medium (**middle**), and low (**bottom**) emissions scenarios, referred as: (**a**) SSP1-2.6 (i.e., emission route that would allow holding global warming to 1.5–2 °C); (**b**) SSP2-4.5 (i.e., scenarios in which every country meets its present goals and commitments under the Paris Climate Agreement); (**c**) SSP5-8.5 (i.e., scenario in which no climate policies are implemented) (Section 2.2.1, Figure 2). Africa's regional differences in projected warming (**left**) and drought (**right**) are more pronounced for the SSP5-8.5 climate change scenario. Source: Own elaboration.

Temperature Projections

The future temperature projections (left panels of Figure 6) indicate an enhanced warming over Africa toward the twenty-first century under all three future scenarios, but the SSP5-8.5 baseline scenario has the most warming (bottom-left panel of Figure 6), which is characterized by high (resp. low) socio-economic challenges to mitigation (resp. adaptation), as it represents a future world characterized by rapid economic expansion, materially intense production and consumption patterns, and a heavy reliance on abundant fossil fuel supplies (Section 2.2.1, Figure 2).

The climate of the African continent varies greatly due to its large latitudinal range, as shown in the left panels of Figure 6. The warming is most pronounced in the northern part of Africa (NAF), which is adjacent to the Mediterranean and Middle Eastern regions, the Sahara (SAH), and the high-elevation areas of South West Africa (SWAF), all of which have been identified as climate change hot spots (except for coastal areas; see the explanation of the land–ocean warming contrast in Section 4.4). The CMIP6 HadGEM3-GC31-LL climate model also projects continuous warming, but with less magnitude, over Central Africa (CAF), North East Africa (NEAF), and South East Africa (SEAF) during the twenty-first century. The lowest values of the mean annual temperature occur over West Africa (WAF) and Central East Africa (CEAF).

Precipitation Projections

On the other hand, the spatial distribution of changes in precipitation during the twenty-first century relative to the reference climate shows large discrepancies over the African continent (right panels of Figure 6). The precipitation projections computed by the CMIP6 HadGEM3-GC31-LL climate model show a reduction and drier conditions over WAF, SWAF, and SEAF, with moderate drought conditions over NAF, and the smallest amount of precipitation occurs in the SSP5-8.5 climate change scenario (bottom-right panel of Figure 6), along with an increasing trend over SAH, NEAF, and CEAF, which have a tendency to wetter conditions and will very likely become prone to flood conditions. Specifically, the mean annual rainfall will decrease by approximately 5–30% and increase by 5–60%. Much higher emission scenario uncertainty in the projected precipitation signal is found over central parts of Africa (CAF), which receive the highest amount of annual rainfall toward the end of the twenty-first century under the SSP5-8.5 scenario (bottom-right panel of Figure 6), which may be related to the Intertropical Convergence Zone (ITCZ) [98].

The explanation of the precipitation patterns in these equatorial and tropical areas can be found in Section 4.8.

3.3.2. Morocco's CMIP6 Climate Projections

Figure 7 shows the CMIP6 climate projections of near-surface air temperature anomaly (°C) over the historical period, depicted in a "black line" (1985–2014) and the future period (2015–2100) according to the three selected scenarios shown in different colors: SSP1-2.6 "green line", SSP2-4.5 "blue line", and SSP5-8.5 "red line"—illustrating the temperature response to both human (e.g., fossil fuel combustion, deforestation) and natural (e.g., solar and volcanic activity) drivers. In fact, each of the three projections prescribes how, among other factors, greenhouse gas emissions and land use could change in the future (Section 2.2.1, Figure 2).

The temperature data are computed as an anomaly at the country scale, that is, the difference from Morocco's average near-surface temperature over the baseline reference period (1850–2014).

Rather than plotting the data from all CMIP6 climate models (Table 1), we instead represent the range of values indicating the spread (uncertainty ranges) across all the models in "gray shading" (Figure 7), as given by quantiles, including the 10th (near the lower limit), the 50th (mid-range), and the 90th (near the upper limit). In fact, a single model run simulates only one possible future climate outcome. In reality, depending on how numerous elements such as greenhouse gas emissions and natural climate variability

change, there are an endless number of conceivable scenarios. This is why climate modelers make projections rather than predictions, stating that in scenario "x", the climate will change in "y" way. The shaded areas in Figure 7 indicate the range of results from all of these distinct climate model runs.

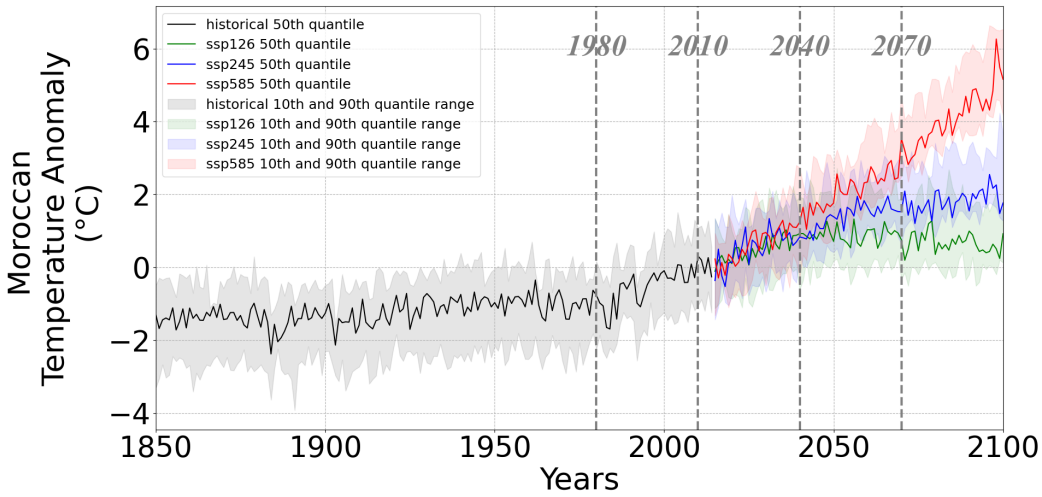

Figure 7. Morocco's CMIP6 annual mean temperature anomaly (°C), in ordinate, over different years, in abscissa, with the black curve representing the historical simulations (1850–2014) and the colors indicating the three Shared Socio-Economic Pathways (SSPs) illustrating different trajectories of future global emissions (2015–2100) and hence challenges to mitigation and adaptation to climate change (Section 2.2.1, Figure 2): SSP1-2.6 (green), SSP2-4.5 (blue), and SSP5-8.5 (red). Each pathway comes with some uncertainty, marked by the gray shading. It represents the spread across all CMIP6 models (Table 1), as given by quantiles: the 10th (near the lower limit), the 50th (mid-range), and the 90th (near the upper limit). The tipping points indicate the near-linear dependence of Morocco's temperature on cumulative greenhouse gas emissions. Source: Own elaboration.

The CMIP6 projections for near-surface air temperature (*circ*C) under low (SSP1-2.6), medium (SSP2-4.5), and high (SSP5-8.5) emission scenarios are presented in three time horizons (Table 2): the historical period (1980–2009), the near future (2010–2039), the mid-future (2040–2069), and the far future (2070–2099).

Table 2. Morocco's climate change signal (°C), computed using CMIP6 climate models (Table 1) as the difference between the near-future (2010–2039), or mid-future (2040–2069), or far-future (2070–2099), and the historical period (1980–2009), under various Shared Socio-Economic Pathways (SSPs) (Section 2.2.1, Figure 2): SSP1-2.6 (i.e., a trajectory of emissions consistent with the Paris Agreement's long-term temperature target), SSP2-4.5 (i.e., scenarios in which the 2030 pledges, known as the Nationally Determined Contributions "NDCs", are achieved), and SSP5-8.5 (i.e., current policies and actions presently in place around the world). Source: Own elaboration.

CMIP6 Models	Hist	SSP1-2.6			SSP2-4.5			SSP5-8.5		
		Near	Mid	Far	Near	Mid	Far	Near	Mid	Far
IPSL-CM6A-LR	20.89	+1.07	+1.69	+1.72	+1.17	+2.41	+3.33	+1.25	+3.18	+6.25
INM-CM4-8	22.46	+0.97	+1.42	+1.18	+1.09	+1.85	+2.34	+1.06	+2.62	+4.39
INM-CM5-0	22.16	+1.05	+1.66	+1.38	+1.16	+2.13	+2.47	+1.3	+2.84	+4.3
MIROC-ES2L	23.60	+1.17	+1.93	+1.83	+1.3	+2.17	+2.93	+1.17	+2.99	+5.16
MPI-ESM1-2-LR	23.03	+0.81	+0.94	+0.89	+0.78	+1.67	+2.13	+0.89	+2.26	+4.31

Figure 7 shows that Morocco's average temperature was more or less stable in the pre-industrial phase but has steadily increased since the 1990s, when Morocco increased its coal capacity and began importing gas from Algeria to displace oil (Chapter 1, Section III, Sub-Section 2 [11]). It shows further that, depending on the SSP scenario, the speed and

increase of Morocco's annual temperature differ. While for the best case SSP1-2.6 scenario, Morocco's annual temperature could stabilize around 1.72 °C, in the worst case SS5-8.5 scenario, Morocco's annual temperature could increase to above 6.25 °C (Table 2, IPSL-CM6A-LR's projections), between the historical baseline period (1980–2009) and the far future (2070–2099).

Overall, the gain of warming in Morocco varies from 0.81 °C to 6.25 °C, depending on the CMIP6 climate model, the scenario, and the time horizon (near-, mid-, or far-future). For instance, according to the IPSL-CM6A-LR CMIP6 climate model, Morocco's mean annual temperature for the near- (resp. long-) term period is projected to increase by approximately 1.07 °C (resp. 1.72 °C), 1.17 °C (resp. 3.33 °C), and 1.25 °C (resp. 6.25 °C) under weak, moderate, and strong forcing, referenced as SSP1-2.6, SSP2-4.5, and SSP5-8.5, respectively (Table 2).

According to Figure 7 and Table 2, to achieve a radiative forcing compatible with the 1.5–2 °C target by the year 2100 (SSP1-2.6, green curve), emissions must be reduced immediately, and even negative emissions must be reached.

Spatio–Seasonal Patterns of Temperature and Precipitation over Morocco

To exhibit the most affected areas with warming and drought in Morocco, we compute the delta changes in seasonal near-surface temperature (°C) climatology (top panel of Figure 8) and seasonal relative change (%) in precipitation climatology (bottom panel of Figure 8) across the four Moroccan sub-regions (bottom-right panel of Figure 1) under the high emissions scenario referred to as SSP5-8.5 (Section 2.2.1, Figure 2) for the future horizon (2015–2100) with 1985–2014 as a reference period.

The climate of Morocco varies greatly from north to south, as shown in Figure 8 (i.e., there are significant spatial discontinuities). The Atlantic Ocean to the west, the Mediterranean Sea to the north, and the Sahara to the south and southeast all have a considerable influence on temperature and rainfall.

The results obtained from the top panel of Figure 8 provide evidence for significant upward warming trends. The grid cells are all red, showing that the country as a whole is becoming hotter. Particularly, it shows that topography exerts a strong influence on the climate-change-induced impacts in Morocco. Coastal areas have lower temperature values than continental areas (i.e., a clear decreasing gradient from east to west). This is due to the sea breezes of the Atlantic Ocean and the Mediterranean Sea. The Atlas and Rif Mountains prevent sea breezes from spreading across the continental areas and hot and dry winds from the south and east from reaching the coast (see an explanation in Section 4.4 and (Chapter 5, Section V, Sub-Section 4 [11])). As can be seen, the temperatures along the Mediterranean and Atlantic coastal lowlands in the North and West are expected to range from 1–3 °C and can reach up 5–6 °C in the interior mountain areas by the late 21st century under the most pessimistic scenario "SSP5-8.5". Thus, the most extreme warming is concentrated over the East and South regions (which indicate an increased risk of heat waves and hence energy demand for air conditioning use), and the warming season extends from July to October. In this context, high-resolution climate simulations are required to reproduce the complex influence of topography on Moroccan climate features (as conducted in (Chapter 5 [11])).

In contrast to warming trends, Morocco's precipitation patterns are highly variable. The bottom panel of Figure 8 shows that the majority of the country's rainfall is expected to fall in the South region between April and June (the spring season), which provides a slightly more intense increase in rainfall compared to other months of the year. A noticeable rise in drought is noted in July and August (the summer season), with the highest drought rates in October that affect the whole country. The drop in rainfall will also be noticed in the autumn and winter, i.e., during the seasons when we regularly record rainfall peaks. This could be linked to changing circulation patterns. In fact, the North Atlantic Oscillation (NAO) is a key atmospheric circulation pattern that influences Moroccan seasonal precipitation [99,100].

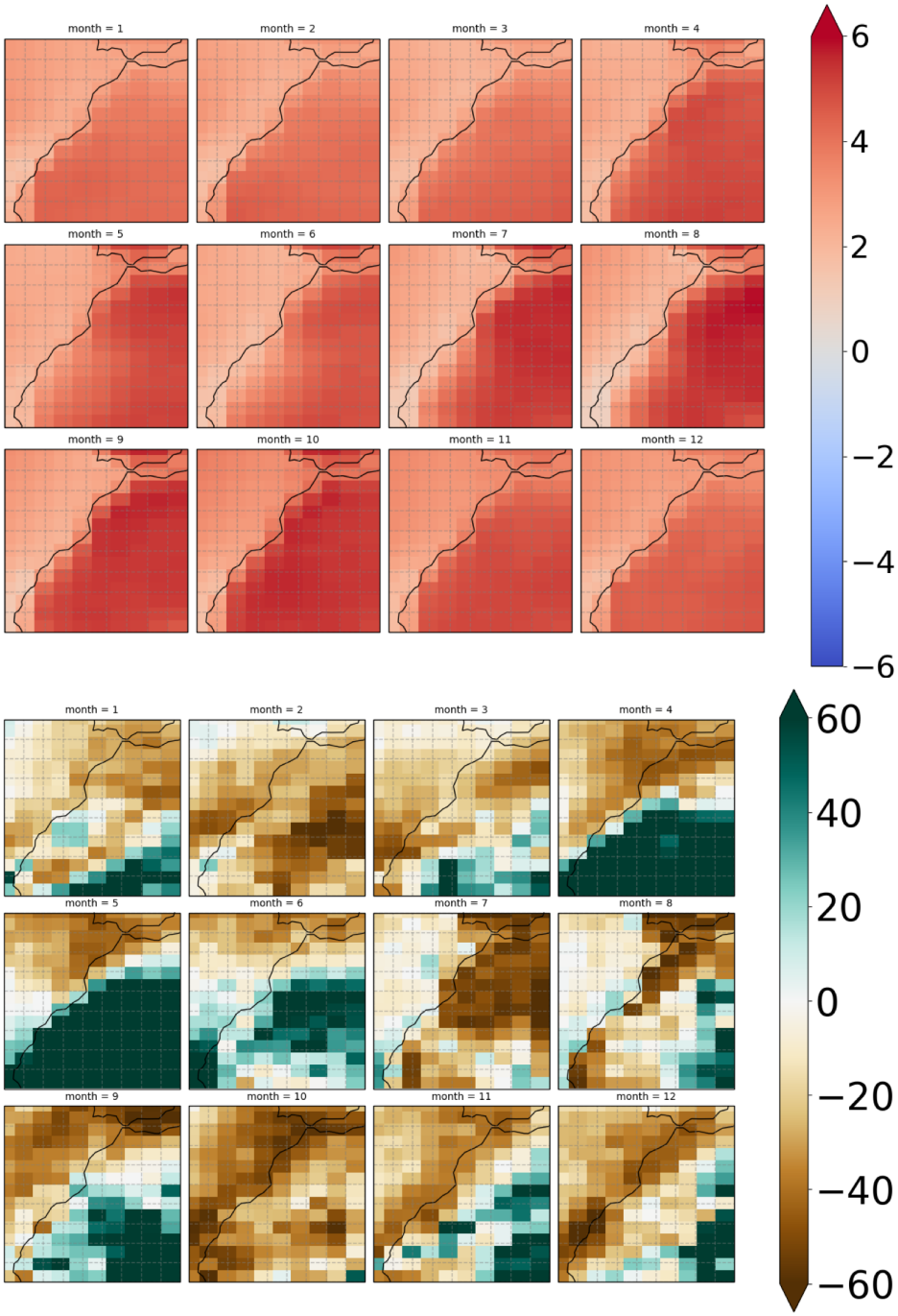

Figure 8. Similar to Figure 6, but numerical simulations are performed for the seasonal change in near-surface temperature (°C) (**top**) and the seasonal relative change (%) in precipitation (**bottom**) across the four Moroccan sub-regions (bottom-right panel of Figure 1), under the high emissions scenario known as SSP5-8.5 (Section 2.2.1, Figure 2). The impact of climate change on Morocco's territory is not uniform and homogeneous and is modulated by topography. Warming rates are expected to be faster in the country's interior (i.e., temperatures typically rise as we move from the coasts to the inland areas), with the South receiving the most rainfall. Source: Own elaboration.

Overall, the southern region of Morocco receives more rainfall than the rest of the country, which can lead to heavy rains and an increased risk of flooding. The results also point to hotter and drier conditions in the other regions (North, East, and West)—areas that currently have higher rainfall. The strong shift from drought to wet events in the South could be attributed primarily to increased moisture in the atmosphere following the

Clausius–Clapeyron relationship of the water holding capacity of air, which increases by approximately 7% per 1 °C warming [101] (see an explanation in Section 3.1.2).

3.4. CMIP5 Versus CMIP6 Climate Projections over Africa and Morocco

We further look at the difference in CMIP5 and CMIP6 climate responses to anthropogenic forcing over Africa and particularly Morocco. To do so, we compute the difference in temperature climatology (°C) (left panels of Figure 9) and the relative change (%) in precipitation (right panels of Figure 9), for 2071–2100 (according to a projected scenario) relative to the reference period (1971–2000) across Africa's eight sub-regions (bottom-left panel of Figure 1), based on the CMIP5 CanRCM4–CanESM2 climate model, considering the medium-low (RCP4.5) (top panels of Figure 9) and strong (RCP8.5) (bottom panels of Figure 9) climate change scenarios.

This allows us to address the fourth fundamental research question of this study (Section 1.4), in which we aim to explore whether future climate projections from the last CMIP (CMIP6) are similar to their CMIP5 predecessors by comparing 30 years of CMIP5 (Figure 9) with the whole period of CMIP6 (Figure 6) temperature (left panels) and precipitation (right panels) projections.

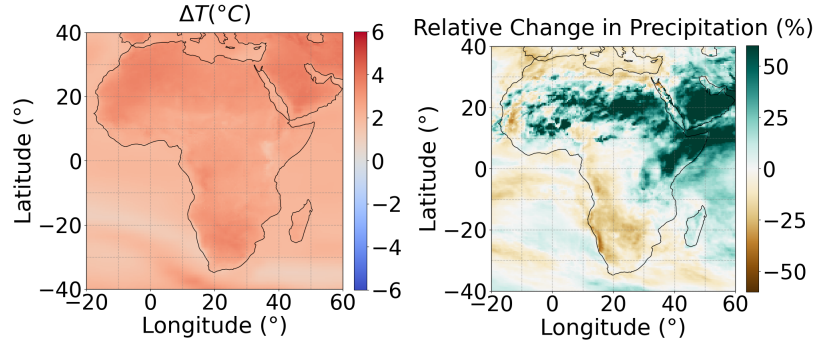

(**a**)

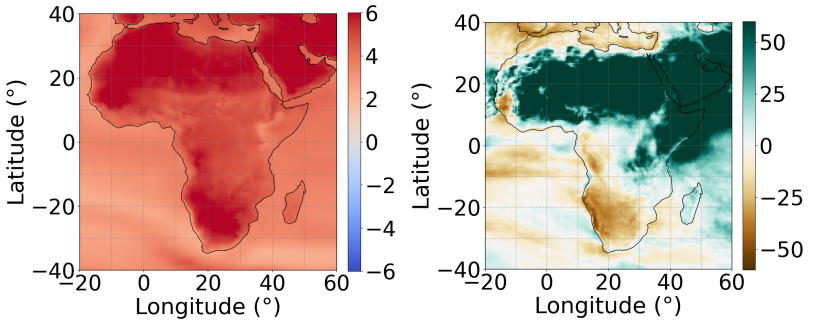

(**b**)

Figure 9. CMIP5 climate change signal, that is, the change in near-surface temperature (°C) climatology (**left**) and the relative change (%) in precipitation climatology (**right**) by the end of this century (2071–2100) relative to the historical reference period (1971–2000) across Africa's eight sub-regions (bottom-left panel of Figure 1) with the longitude (°), in abscissa, and the latitude (°), in ordinate. Data are from the CanRCM4-CanESM2 climate model under the medium-low (**top**) and high-end (**bottom**) emissions scenarios, referred to as (**a**) RCP4.5 and (**b**) RCP8.5 (Section 2.2.2). The variation over time is depicted in color by the intensity of the color bar, with temperature (resp. precipitation) increasing in red (resp. green) and decreasing in blue (resp. brown). We compute the difference between the two climatologies by subtracting the historical climatology from the projected climatology. To be compared with Figure 6. Source: Own elaboration.

Within each CMIP, there are no significant regional discrepancies between the two future temperature and rainfall estimates. However, we note that for both scenarios, the CMIP5 CanRCM4–CanESM2 climate model (Figure 9) simulates higher temperatures and drought over large parts of Africa compared to the CMIP6 HadGEM3-GC31-LL model (Figure 6), with some differences over the areas surrounding the SEAF, but the differences are not significant elsewhere. This could be due to the CMIP5's short historical and future timeframe of only 30 years, which is insufficient to draw firm conclusions because the model's inherent variability can have a relevant effect on timescales.

Overall, differences between the CMIP5 and CMIP6 climate models are obscured by inherent differences in the primary atmospheric circulation mechanisms occurring in each region, as well as differences in uncertainty between regions. In fact, the CMIP6 dataset differs from the previous generation (i.e., CMIP5 [30]) because CMIP6 used updated versions of the coupled global climate models with higher resolution [102], a new start year, and a new set of Shared Socio-Economic Pathways (SSP) scenarios of concentrations [103]. It would be interesting to discover the reasons for the divergent response of specific areas in the two CMIPs in follow-up analyses, as provided in [104,105].

4. Summary and Discussion

4.1. Research Motivation

Climate change is expected to significantly impact the world in multiple dimensions. For its part, Africa, and particularly Morocco, is not immune to the climate change phenomenon and cannot deal alone with its controversial political decisions.

4.2. Methodology

Data from the Coupled Model Intercomparison Project Phase 6 (CMIP6) climate models (Table 1) are used in this investigation to assess the future changes in temperature and precipitation and the level of consistency in climate projections over the world and particularly over Africa's and Morocco's sub-regions (Figure 1). Three Shared Socio-Economic Pathway (SSP) scenarios (SSP1-2.6, SSP2-4.5, and SSP5-8.5), depicting various future greenhouse gas (GHG) emissions and land use ranges (Figure 2), are employed to project change during one time horizon (2015–2100) relative to the historical baseline period (1850–2014), considering annual and seasonal patterns. To further assess the accuracy of the estimates, we compare the results to climate scenarios from the COordinated Regional climate Downscaling EXperiment (CORDEX)-CMIP5 climate model, whose projections are based on the Representative Concentration Pathway (RCP) scenarios, RCP4.5 and RCP8.5, by the end of the twenty-first century (2071–2100) relative to the historical reference forcing (1971–2000) over Africa (Section 2.2.2).

4.3. General Findings

We find that land areas are warmer than ocean areas. Global climate models project that the Arctic will see a stronger surface warming than Antarctica, and both are warming up considerably faster than the rest of the Earth, mainly because of differences in how these areas reflect energy from the sun (top panel of Figure 3).

The highest rainfall areas are located in the equatorial zones and Asia's monsoon zones. Similarly, most of the increase in rainfall is projected to occur in the high latitudes. Little rain falls in the desert regions of the subtropics compared to the mid-latitudes, which receive moderate amounts of precipitation (bottom panel of Figure 3).

While CMIP6 climate models generally project high levels of committed warming and drought in the future, there is much less agreement on the magnitude of these changes. For instance, depending on the model, the same location could become significantly wetter or dryer under the SSP2-4.5 global warming scenario (Figures 3–5). However, results are not only influenced by model uncertainty but also by uncertainty pertaining to forcing conditions, the climate system's intrinsic variability, and the intra-daily parametrization of climate variables of relevance for renewable production and electricity consumption, which

is not resolved by CMIP5/6 projections (see discussion on the sources of uncertainties associated with future energy mixes in (Chapter 5 [11]) which is also raised in [106]).

Projected temperature and precipitation over Africa show substantial spatial variability during the twenty-first century. The northern part of Africa (NAF), the Sahara (SAH), and South West Africa (SWAF) are projected to undergo increasing warming, followed by Central Africa (CAF), North East Africa (NEAF), and South East Africa (SEAF). West Africa (WAF) and Central East Africa (CEAF) will experience the lowest values of mean annual temperature compared with other regions (left panels of Figure 6).

Results show that the SAH, NEAF, and CEAF are expected to receive strong precipitation relative to the NAF, WAF, SWAF, and SEAF, which are likely to experience severe drought conditions. The emission scenario has a significant impact on the amount of rain that falls over Central Africa (CAF), which displays enhanced precipitation under SSP5-8.5 (right panels of Figure 6).

While the methodology and CMIP6 climate models used in this study differ, there is consistency with the general finding of Almazroui et al. [64].

Morocco's climate is changing and is projected to continue to do so across all emission scenarios through the end of this century.

The amount of greenhouse (heat-trapping) gases emitted globally over the coming decades (i.e., emission scenario) and the level of uncertainty in Morocco's climate sensitivity to those emissions (i.e., climate model, time horizon) will determine the extent of climate change beyond the next few decades. With significant reductions in greenhouse gas (GHG) emissions, "SSP1-2.6", we find that Morocco's annual averaged temperature rise, for the near- (resp. long)-term period, could be limited to 1.07 °C (resp. 1.72 °C). However, if these emissions are not significantly reduced, "SSP5-8.5", the increase in annual average temperatures relative to baseline times might reach 1.25 °C (resp. 6.25 °C) by the end of the century (Figure 7 and Table 2).

Morocco's spatio–seasonal warming pattern is strongest in the mountainous areas of the Rif and Atlas Mountains and weakens along the coastal areas of the Atlantic Ocean and the Mediterranean Sea (top panel of Figure 8). The findings also show a significant gradual appearance of humid climate in the South region, as well as a migration of aridity to the North, East, and West regions (bottom panel of Figure 8).

Driouech et al. [56], Ait Brahim et al. [57], Filahi et al. [58], and Bouramdane et al. (Chapter 5 [11]) reported similar results concerning the heterogeneous spatial distribution of Morocco's climate-change-induced impacts (i.e., regions with marked increases in temperature and pronounced decreases in mean precipitation), which is related to the topography and the difference between the coastal and inland areas (Section 2.1).

Across both medium and high emission scenarios, the CMIP6 warming and drought closely follow the CMIP5 median warming lines, but less so on the magnitude of changes. CMIP5 seems to be the one with the highest warming estimation, as the warming tendency becomes more visible towards the end of the current century (Figures 6 and 9).

4.4. Why Does Land Warm Up Faster than Oceans?

A possible explanation of this land–ocean warming contrast (Section 3.1.1) would be the contrasting heat capacity and lapse rate changes over land surfaces and oceans. In fact, under scenarios of climate change where CO_2 emissions increase, a considerable portion of the heat generated by the Earth's surface is retained in the atmosphere by greenhouse gases, causing temperatures to rise. However, the intensity of this CO_2-induced surface warming is determined by how much is offset by localized cooling factors. Oceans have an infinite amount of water to evaporate (i.e., at any given time, the air above the ocean contains more water vapor than the air above land), a high heat capacity (i.e., the product of specific heat and mass), and reflect the majority of solar radiation that reaches their surface back into the atmosphere. Land surfaces, or continents, on the other hand, retain more heat (i.e., it takes less heat to warm land than water) and have limited moisture availability. Hence, evaporation is constrained. The drier the land is, the more it warms.

This explains why land warming will be especially severe in dry and arid subtropical regions [107]. Furthermore, a slower fall in land lapse rate—the rate at which temperature decreases with height—implies a rapid increase in land surface temperature relative to the freely evaporating oceans, which undergo temperature changes whose amplitude is less than that of the surrounding continents (top panel of Figure 3).

Regional topography influences this too. Indeed, mountains and high-elevation locations are particularly vulnerable to future climate change [108].

4.5. Why Do the Poles, Particularly the North Pole (Arctic), Tend to Warm Faster Than the Rest of the Planet?

An explanation of this tendency, shown in the top panel of Figure 3, is the melting of the ice, as the white pack ice has the particularity of reflecting the sun's rays. In fact, the reflective power of this surface is known as "albedo". It expresses the part of solar radiation that will be sent back to the atmosphere and that will not be used to heat the planet. The albedo is expressed as a percentage—the amount of light reflected by the surface in comparison to the amount it receives. Ice has an albedo of around 60%, while that of snow can be up to 90%. When pack ice melts, it changes the albedo, which changes the energy exchanges on Earth. In fact, as the ice melts, it gives way to a darker ocean. This absorbs more solar heat than the pack ice—its albedo is between 5 and 10%. This heat absorption reduces the likelihood of sea ice renewal and increases the likelihood that global warming will accelerate. Finally, the situation produces a loop system: the absorption of heat causes temperatures to rise, which themselves accentuate the melting of the ice and therefore the reduction in their albedo [109,110]. In addition, the warming of the poles is encouraged by another element: the displacements of heat that take place in the atmosphere and oceans in the direction of the poles [111].

Indeed, this warming disparity between the poles and the tropics is referred to as Arctic (or polar) amplification [112]. It occurs whenever the Earth's net radiation balance changes, resulting in a greater shift in temperature near the poles than the global average. Some studies have linked the rapid Arctic warming to mid-latitude weather patterns [113,114] and shifts in cloud patterns [115].

4.6. Is Antarctica Experiencing the Same Thing?

The term "polar amplification" can be used to describe the greater climate change at the poles. As can be seen in the top panel of Figure 3, polar amplification in the Arctic is substantially stronger than in Antarctica. This is because the Arctic is an ocean surrounded by land and covered by a thin coating of sea ice. Antarctica, on the other hand, is a continent, surrounded by sea ice and covered by a thick ice cap. As a result of its massive ice cover and high temperatures, the white continent is less affected by global warming than the North Pole.

4.7. What Are the Reasons for Different Rainfall Patterns?

In fact, the water-holding capacity of air increases with increasing temperature, particularly over oceans. According to the Clausius–Clapeyron relationship, saturated air contains 7% more water vapor for every 1 °C of global warming [116]. As a result, a world that is around 2.7 °C (SSP2-4.5 emission scenario) warmer than the pre-industrial era will have around 19% greater atmospheric water content. However, the increased moisture is not uniformly distributed over the Earth. As weather patterns and the customary locations of rain belts and deserts fluctuate in reaction to climate change, some areas may see heavier-than-normal precipitation, while others are projected to become prone to drought. If the Earth's surface were absolutely uniform, long-term average rainfall would be spread in discrete latitudinal bands; however, the pattern of global winds, the distribution of land and sea, and the presence of mountains complicate the issue. Because rainfall occurs as a result of the ascent and cooling of wet air, places of heavy rain imply rising air, whereas deserts occur in locations where the air is warmed and dried during its descent. On average,

in a future warming climate, evaporation will be enhanced, which decreases surface water and dries up soils and vegetation, causing dry areas to become drier and wet regions to become wetter (bottom panel of Figure 3).

4.8. Why Do the Equatorial Regions and Some Areas in the Tropics Receive a Lot of Precipitation?

One explanation is that the equatorial regions receive a lot of direct solar energy, which causes more evaporation than higher latitudes. Warm, moist air rises, condenses into clouds and thunderstorms and then falls back to Earth as precipitation. Increased evaporation leads to more precipitation (approximately 30–60% wetter, bottom panel of Figure 3).

In fact, trade winds from both hemispheres converge in the equatorial belt, causing a general upward motion of air that becomes amplified locally in tropical storms that generate exceptionally heavy rainfall in these locations.

4.9. Why Is There a Lack of Rainfall in Deserts?

In fact, while some deserts are extremely hot, others endure cold winters or are frozen all year. One thing all deserts have in common is that they are arid, or dry. Deserts are classified into five types: subtropical, coastal, rain-shadow, interior, and polar. Deserts are classified into several groups based on the causes of their aridity.

The circulation patterns of air masses generate subtropical deserts. They are found between 15 and 30 degrees north of the equator along the Tropic of Cancer or between 15 and 30 degrees south of the equator along the Tropic of Capricorn. Because the air is hot, most of it rises into the atmosphere around the Equator. As the air rises, it cools and releases moisture in the form of strong tropical rains. The cooler, drier air mass that results moves away from the Equator. The air descends and warms up again when it approaches the tropics. Because the descending air prevents clouds from forming, very little rain falls on the ground below. The Sahara, the world's largest hot desert, is a subtropical desert in northern Africa. The Kalahari Desert in southern Africa and the Tanami Desert in northern Australia are other subtropical deserts.

Cold ocean currents contribute to the formation of coastal deserts. A layer of fog forms when air blows toward the shore and is chilled by contact with cold water. This dense fog drifts onto land. Despite the high humidity, the atmospheric shifts that normally induce rainfall are absent. A coastal desert may be nearly rainless but fogged in. The Atacama Desert, located on Chile's Pacific coast, is a coastal desert. Fog frequently blankets parts of the Atacama Desert. However, the region can endure for decades without rain. In fact, the Atacama Desert is the world's driest place.

Some mountain ranges have rain-shadow deserts on their leeward slopes. Leeward slopes are those that face away from the prevailing winds. When moist air collides with a mountain range, it is forced to rise. The air then cools and condenses to produce clouds, which drop rain on windward (windward-facing) slopes. There is little moisture left when the air flows over the peak and begins to descend the leeward slopes. The falling air heats up, making cloud formation difficult. Death Valley, located in California and Nevada, is a rain-shadow desert. The Sierra Nevada mountains cast a rain shadow over Death Valley, the lowest and driest area in North America.

Interior deserts exist in the centers of continents because moisture-laden breezes do not reach them. Coastal air masses have lost all of their moisture by the time they reach the interior. Interior deserts are also known as "inland deserts". The Gobi Desert, which stretches across China and Mongolia, is hundreds of kilometers from the sea. The moisture in the winds that reach the Gobi has long since evaporated. In addition, the Gobi is in the rain shadow of the Himalaya Mountains to the south.

Deserts can be found in parts of the Arctic and Antarctica. These arctic deserts contain a lot of water, but most of it is trapped in glaciers and ice sheets all year. The world's largest desert is also the coldest. Almost the whole Antarctic continent is a polar desert with little precipitation (in some places, the bottom panel of Figure 3).

4.10. How about the Precipitation Patterns in High and Middle Latitudes?

More severe precipitation can be produced when more moisture-laden air flows over land or converges into a storm system (i.e., heavier rain and snowstorms). Increased snowfall near both poles may offset some of the melting of glaciers and ice sheets in these places by depositing new ice on their tops. Some areas of Antarctica may gain more snow as a result of higher precipitation than they lose due to melting induced by rising temperatures. Taken together, these findings suggest that there is a link between changes in precipitation and levels of warming (see discussion in Section 3.1.1).

Weather and rainfall in the mid-latitudes are dominated by migrating depressions and fronts that provide a significant amount of rain in all seasons and in most places, with the exception of some areas of the Asian and North American continents.

4.11. Sources of Uncertainty Associated with Future Projections

Yet, despite climate models becoming increasingly complex and sophisticated in simulating the Earth's climate, scientists are still struggling with a lack of or low-quality data in many areas. This affects their ability to understand various aspects of the climate system, to estimate trends in the occurrence of droughts, etc.; hence, it is difficult to validate climate models. This is especially true at the regional scale, where the local climate's specifics are inherently chaotic. As a result, it is strongly recommended that analysis use multi-model ensembles unless the underlying assumptions and biases of each individual model are thoroughly understood (see discussion in Section 4.12).

The accuracy of climate projections is also dependent on the different scenarios of future socio-economic development that go into them (e.g., if greenhouse gas emissions will fall or increase). This adds another layer of uncertainty to projections.

Understanding whether "change" is a result of natural variability (i.e., the coupled atmosphere–ocean-land–ice system's quasi-random internal variability) and periodic "forcing" events of non-human nature (i.e., volcanic eruption or solar activity) or whether projected change reveals trends that are statistically significant from natural variability is crucial to projecting climate change.

4.12. Originality of This Study, Limitations, and Implications

The analysis of climate change around the world allows for a more comprehensive study of the climate signal in different regions because, as stated previously, although climate change is a worldwide concern, its impacts are not the same everywhere. Each continent, country, and region will be affected differently. These consequences include varying rates of warming and drought. Because the climate is global, what happens in other locations can have an impact on where we live. Additionally, it is possible to understand why similarly forced models produce a range of responses in different locations by comparing different CMIP6 climate models. The disagreement that we find in the intensity of the climate change signal (Section 3.2) means that the changes in temperature and precipitation projected by climate models remain highly uncertain, despite scientific advances. In fact, climate models are limited in important ways (i.e., an imperfect ability to transform our knowledge of the climate system into accurate mathematical equations, etc.). This presents a challenge for decision makers who must foresee changes that will occur in their country. However, the usefulness of climate model simulations cannot be inferred solely from their degree of agreement in the magnitude of future temperature and rainfall changes, as they nearly tell the same story about future changes (Figures 3–5). In fact, for the sake of simplicity and to facilitate data download, this study makes use of some of the coarser resolution models that have a smaller data size. It is, nevertheless, only a choice for this research and not a recommendation, since ideally all climate models, including those with the highest resolution, should be used for a more reliable output (Section 2.2).

To conclude, this study is one of the preliminary evaluations of CMIP6 climate models on Africa and is the first study on Morocco. It provides useful information regarding regional temperature and precipitation trends and can be used as a reference for the

Food–Energy–Water Nexus, offering firsthand knowledge on impacts (including seasonal changes), shedding light on land–ocean warming contrast, polar amplification, reasons for different rainfall patterns (in the equatorial and tropical regions compared to deserts and high and middle latitudes), the sources of inconsistencies in the results generated based on different climate models, and highlighting the changes from RCP-based scenarios for CMIP5 and SSP-based scenarios for CMIP6.

Funding: This article is not part of any project and received no external funding.

Institutional Review Board Statement: Not applicable.

Informed Consent Statement: Not applicable.

Data Availability Statement: The data used in this study are available upon reasonable request to the author.

Acknowledgments: We acknowledge the World Climate Research Programme's Working Group on Coupled Modeling, which is responsible for the Coupled Model Intercomparison Project (CMIP), and we thank the climate modeling groups (listed in Table 1 or in general in Section 2.2) for producing and making available their model outputs. For CMIP, the U.S. Department of Energy's Program for Climate Model Diagnosis and Intercomparison provides coordination support and software development leadership infrastructure in partnership with the Global Organization for Earth System Science Portals. We are also grateful to the reviewers for their careful review and positive comments.

Conflicts of Interest: The author declares no conflict of interest.

References

1. IPCC. *Climate Change 2007: Synthesis Report. Contribution of Working Groups I, II and III to the Fourth Assessment Report of the Intergovernmental Panel on Climate Change*; Core Writing Team, Pachauri, R.K., Reisinger, A. Eds.; IPCC: Geneva, Switzerland, 2007. Available online: https://www.ipcc.ch/site/assets/uploads/2018/02/ar4_syr_full_report.pdf (accessed on 25 December 2022).
2. IPCC. *Climate Change 2014: Synthesis Report. Contribution of Working Groups I, II and III to the Fifth Assessment Report of the Intergovernmental Panel on Climate Change*; Core Writing Team, Pachauri, R.K., Meyer, L.A., Eds.; IPCC: Geneva, Switzerland, 2014. Available online: https://www.ipcc.ch/site/assets/uploads/2018/05/SYR_AR5_FINAL_full_wcover.pdf (accessed on 25 December 2022).
3. IPCC. Summary for Policymakers. In *Climate Change 2021: The Physical Science Basis. Contribution of Working Group I to the Sixth Assessment Report of the Intergovernmental Panel on Climate Change*; Masson-Delmotte, V., Zhai, P., Pirani, A., Connors, S.L., Péan, C., Berger, S., Caud, N., Chen, Y., Goldfarb, L., Gomis, M.I., et al., Eds.; IPCC: Geneva, Switzerland; Cambridge University Press: Cambridge, UK; Cambridge University Press: New York, NY, USA, 2021. Available online: https://www.ipcc.ch/report/ar6/wg1/downloads/report/IPCC_AR6_WGI_SPM.pdf (accessed on 25 December 2022).
4. Berger, A.; Maracchi, G.; Teixeira, M. Milankovitch Effects on Long-Term Climatic Changes. 1991. Available online: https://core.ac.uk/download/pdf/15490045.pdf (accessed on 25 December 2022).
5. Bouramdane, A.A. Chaleur Caniculaire, Incendies Gigantesques à Répétition: Des Signes du Changement Climatique? *énergies/mines carrières* **2022**. [CrossRef]
6. Bouramdane, A.A. Sécheresse: L'extrême va-t-il progressivement devenir la norme? *énergies/mines carrières* **2022**. [CrossRef]
7. Yalew, S.G.; van Vliet, M.T.H.; Gernaat, D.E.; Ludwig, F.; Miara, A.; Park, C.; Byers, E.A.; Cian, E.D.; Piontek, F.; Iyer, G.C.; et al. Impacts of Climate Change on Energy Systems in Global and Regional Scenarios. *Nat. Energy* **2020**, *5*, 794–802. [CrossRef]
8. Dasgupta, S.; van Maanen, N.; Gosling, S.N.; Piontek, F.; Otto, C.; Schleussner, C.F. Effects of Climate Change on Combined Labour Productivity and Supply: An Empirical, Multi-Model Study. *Lancet Planet. Health* **2021**, *5*, e455–e465. [CrossRef] [PubMed]
9. IPCC. *Climate Change 1995: Economic and Social Dimensions of Climate Change. Contribution of Working Group III to the Second Assessment Report of the Intergovernmental Panel on Climate Change*; IPCC: Geneva, Switzerland; Cambridge University Press: Cambridge, UK; Cambridge University Press: New York, NY, USA, 1995. Available online: https://www.ipcc.ch/site/assets/uploads/2018/03/ipcc_sar_wg_III_full_report.pdf (accessed on 25 December 2022).
10. Bouramdane, A.A. PV, CSP et Éolien au Maroc: Intégration à Géométrie Variable. *énergies/mines carrières* **2022**. [CrossRef]
11. Bouramdane, A.A. Scenarios of Large-Scale Solar Integration with Wind in Morocco : Impact of Storage, Cost, Spatio-Temporal Complementarity and Climate Change. Ph.D. Thesis, Institut Polytechnique de Paris, Palaiseau, France, 2021.
12. Bouramdane, A.A.; Tantet, A.; Drobinski, P. Adequacy of Renewable Energy Mixes with Concentrated Solar Power and Photovoltaic in Morocco: Impact of Thermal Storage and Cost. *Energies* **2020**, *13*, 5087. [CrossRef]
13. Bouramdane, A.A.; Tantet, A.; Drobinski, P. Utility-Scale PV-Battery versus CSP-Thermal Storage in Morocco: Storage and Cost Effect under Penetration Scenarios. *Energies* **2021**, *14*, 4675. [CrossRef]

14. Bouramdane, A.A.; Tantet, A.; Drobinski, P. Sensitivity of the Moroccan Mix to the Integration of Thermal and Battery Storage Combined with Concentrated Solar Power and Photovoltaics: Design, Dispatch and Optimal Mix Analysis. In Proceedings of the EGU General Assembly 2021, EGU21-8755, online, 19–30 April 2021. [CrossRef]
15. Bouramdane, A.A. Pourquoi l'Attenuation et l'Adaptation aux Changements Climatiques sont Complementaires? *énergies/mines carrières* **2022**. [CrossRef]
16. Tol, R.S.J. Adaptation and Mitigation: Trade-Offs in Substance and Methods. *Environ. Sci. Policy* **2003**, *8*, 572–578. [CrossRef]
17. Bouramdane, A.A. Agrivoltaïque, De Quoi Parle-t-on Au Juste? *énergies/mines carrières* **2022**, zenodo.7324691. [CrossRef]
18. Barron-Gafford, G.A.; Pavao-Zuckerman, M.A.; Minor, R.L.; Sutter, L.F.; Barnett-Moreno, I.; Blackett, D.; Thompson, M.; Dimond, K.; Gerlak, A.K.; Nabhan, G.P.; et al. Agrivoltaics Provide Mutual Benefits Across the Food–Energy–Water Nexus in Drylands. *Nat. Sustain.* **2019**, *2*, 848–855. [CrossRef]
19. Bundschuh, J.; Kaczmarczyk, M.; Ghaffour, N.; Tomaszewska, B. State-of-the-Art of Renewable Energy Sources Used in Water Desalination: Present and Future Prospects. *Desalination* **2021**, *508*, 115035. [CrossRef]
20. Curto, D.; Franzitta, V.; Guercio, A. A Review of the Water Desalination Technologies. *Appl. Sci.* **2021**, *11*, 670. [CrossRef]
21. Continents by Population 2021—StatisticsTimes.com. Available online: https://statisticstimes.com/index.php (accessed on 25 December 2022)
22. Thomas, D.S.G.; Twyman, C. Equity and Justice in Climate Change Adaptation Amongst Natural-Resource-Dependent Societies. *Glob. Environ. Chang.-Hum. Policy Dimens.* **2005**, *15*, 115–124. [CrossRef]
23. Desanker, P. Impact of Climate Change on Life in Africa. 2002. Available online: https://wwflac.awsassets.panda.org/downloads/wwfbinaryitem4926.pdf (accessed on 25 December 2022).
24. Morocco's Nationally Determined Contribution Under the UNFCCC. Available online: https://www4.unfccc.int/sites/ndcstaging/PublishedDocuments/Morocco%20First/Morocco%20First%20NDC-English.pdf (accessed on 21 June 2021).
25. IEA. Energy Policies Beyond IEA Countries: Morocco 2019. 2019. Available online: https://www.connaissancedesenergies.org/sites/default/files/pdf-actualites/Energy_Policies_beyond_IEA_Contries_Morocco.pdf (accessed on 25 December 2022).
26. CAT (Climate Action Tracker). Available online: https://climateactiontracker.org (accessed on 25 December 2022).
27. Schilling, J.; Freier, K.P.; Hertig, E.; Scheffran, J. Climate Change, Vulnerability and Adaptation in North Africa with Focus on Morocco. *Agric. Ecosyst. Environ.* **2012**, *156*, 12–26. [CrossRef]
28. Meehl, G.A.; Covey, C.; Delworth, T.L.; Latif, M.; Mcavaney, B.J.; Mitchell, J.F.B.; Stouffer, R.J.; Taylor, K.E. THE WCRP CMIP3 Multimodel Dataset: A New Era in Climate Change Research. *Bull. Am. Meteorol. Soc.* **2007**, *88*, 1383–1394. [CrossRef]
29. Nakicenovic, N.; Alcamo, J.; Davis, G.; de Vries, B.; Fenhann, J.V.; Gaffin, S.R.; Gregory, K.; Grubler, A.; Jung, T.Y.; Kram, T.; et al. Special Report on Emissions Scenarios: A Special Report of Working Group III of the Intergovernmental Panel on Climate Change. 2000. Available online: https://www.ipcc.ch/site/assets/uploads/2018/03/emissions_scenarios-1.pdf (accessed on 25 December 2022).
30. Taylor, K.E.; Stouffer, R.J.; Meehl, G.A. An Overview of CMIP5 and the Experiment Design. *Bull. Am. Meteorol. Soc.* **2012**, *93*, 485–498. [CrossRef]
31. Stocker, T.; Qin, D.; Plattner, G.; Tignor, M.; Allen, S.; Boschung, J.; Nauels, A.; Xia, Y.; Bex, V.; Midgley, P.; et al. Climate Change 2013. The Physical Science Basis. Working Group I Contribution to the Fifth Assessment Report of the Intergovernmental Panel on Climate Change—Abstract For Decision-Makers. 2013. Available online: https://www.ipcc.ch/site/assets/uploads/2017/09/WG1AR5_Frontmatter_FINAL.pdf (accessed on 25 December 2022).
32. Vuuren, D.; Edmonds, J.; Kainuma, M.; Riahi, K.; Thomson, A.; Hibbard, K.; Hurtt, G.; Kram, T.; Krey, V.; Lamarque, J.; et al. The Representative Concentration Pathways: An Overview. *Clim. Chang.* **2011**, *109*, 5–31. [CrossRef]
33. Moss, R.; Edmonds, J.; Hibbard, K.; Manning, M.; Rose, S.; Vuuren, D.; Carter, T.; Emori, S.; Kainuma, M.; Kram, T.; et al. The Next Generation of Scenarios For Climate Change Research and Assessment. *Nature* **2010**, *463*, 747–756. [CrossRef] [PubMed]
34. Eyring, V.; Bony, S.; Meehl, G.A.; Senior, C.A.; Stevens, B.; Stouffer, R.J.; Taylor, K.E. Overview of the Coupled Model Intercomparison Project Phase 6 (CMIP6) Experimental Design and Organization. *Geosci. Model Dev.* **2015**, *9*, 1937–1958. [CrossRef]
35. O'Neill, B.C.; Tebaldi, C.; van Vuuren, D.P.; Eyring, V.; Friedlingstein, P.; Hurtt, G.C.; Knutti, R.; Kriegler, E.; Lamarque, J.; Lowe, J.A.; et al. The Scenario Model Intercomparison Project (ScenarioMIP) for CMIP6. *Geosci. Model Dev.* **2016**, *9*, 3461–3482. [CrossRef]
36. O'Neill, B.C.; Kriegler, E.; Ebi, K.L.; Kemp-Benedict, E.; Riahi, K.; Rothman, D.S.; van Ruijven, B.J.; van Vuuren, D.; Birkmann, J.; Kok, K.; et al. The Roads Ahead: Narratives for Shared Socioeconomic Pathways Describing World Futures in the 21st Century. *Glob. Environ. Chang.-Hum. Policy Dimens.* **2017**, *42*, 169–180. [CrossRef]
37. Císcar, J.C.; Dowling, P.M. Integrated Assessment of Climate Impacts and Adaptation in the Energy Sector. *Energy Econ.* **2014**, *46*, 531–538. [CrossRef]
38. Bosetti, V. Integrated Assessment Models for Climate Change. 2021. Available online: https://oxfordre.com/economics/display/10.1093/acrefore/9780190625979.001.0001/acrefore-9780190625979-e-572;jsessionid=5850E6B1195C219958452862F877870D (accessed on 25 December 2022).
39. Li, C.; Zwiers, F.W.; Zhang, X.; Li, G.; Sun, Y.; Wehner, M.F. Changes in Annual Extremes of Daily Temperature and Precipitation in CMIP6 Models. *J. Clim.* **2020**, *34*, 3441–3460. [CrossRef]

40. Zhai, J.; Mondal, S.K.; Fischer, T.; Wang, Y.; Su, B.; Huang, J.; Tao, H.; Wang, G.; Ullah, W.; Uddin, M.J. Future Drought Characteristics Through a Multi-Model Ensemble from CMIP6 over South Asia. *Atmos. Res.* **2020**, *246*, 105111. [CrossRef]
41. Liu, F.; Xu, C.; Long, Y.; Yin, G.; Wang, H. Assessment of CMIP6 Model Performance for Air Temperature in the Arid Region of Northwest China and Subregions. *Atmosphere* **2022**, *13*, 454. [CrossRef]
42. Shrestha, A.; Rahaman, M.M.; Kalra, A.; Jogineedi, R.; Maheshwari, P. Climatological Drought Forecasting Using Bias Corrected CMIP6 Climate Data: A Case Study for India. *Forecasting* **2020**, *2*, 59–84. [CrossRef]
43. Almazroui, M.; Islam, M.N.; Saeed, F.; Saeed, S.; Ismail, M.F.; Ehsan, M.A.; Diallo, I.; O'Brien, E.; Ashfaq, M.; Martínez-Castro, D.; et al. Projected Changes in Temperature and Precipitation Over the United States, Central America, and the Caribbean in CMIP6 GCMs. *Earth Syst. Environ.* **2021**, *5*, 3441–3460. [CrossRef]
44. Monteverde, C.; Sales, F.D.; Jones, C. Evaluation of the CMIP6 Performance in Simulating Precipitation in the Amazon River Basin. *Climate* **2022**, *10*, 122. [CrossRef]
45. Babaousmail, H.; Ayugi, B.O.; Rajasekar, A.; Zhu, H.; Oduro, C.; Mumo, R.; Ongoma, V. Projection of Extreme Temperature Events over the Mediterranean and Sahara Using Bias-Corrected CMIP6 Models. *Atmosphere* **2022**, *13*, 741. [CrossRef]
46. Seneviratne, S.I.; Hauser, M. Regional Climate Sensitivity of Climate Extremes in CMIP6 Versus CMIP5 Multimodel Ensembles. *Earth's Future* **2020**, *8*, e2019EF001474. [CrossRef]
47. Cos, J.; Doblas-Reyes, F.J.; Jury, M.W.; Marcos, R.; Bretonnière, P.A.; Samsó, M. Supplementary Material to "The Mediterranean Climate Change Hotspot in the CMIP5 and CMIP6 Projections". *Earth Syst. Dyn.* **2021**, *13*, 321–340. [CrossRef]
48. Hamed, M.M.; Nashwan, M.S.; Shiru, M.S.; Shahid, S. Comparison between CMIP5 and CMIP6 Models over MENA Region Using Historical Simulations and Future Projections. *Sustainability* **2022**, *14*, 10375. [CrossRef]
49. Monerie, P.; Wainwright, C.M.; Sidibe, M.F.; Akinsanola, A.A. Model Uncertainties in Climate Change Impacts on Sahel Precipitation in Ensembles of CMIP5 and CMIP6 Simulations. *Clim. Dyn.* **2020**, *55*, 1385–1401. [CrossRef]
50. Kamruzzaman, M.; Shahid, S.; Islam, A.T.; Hwang, S.; Cho, J.P.; Zaman, M.A.U.; Ahmed, M.U.; Rahman, M.M.; Hossain, M.B. Comparison of CMIP6 and CMIP5 Model Performance in Simulating Historical Precipitation and Temperature in Bangladesh: A Preliminary Study. *Theor. Appl. Climatol.* **2021**, *145*, 1385–1406. [CrossRef]
51. Palmer, T.E.; Booth, B.B.B.; McSweeney, C.F. How Does the CMIP6 Ensemble Change the Picture for European Climate Projections? *Environ. Res. Lett.* **2020**, *16*, 094042. [CrossRef]
52. Narsey, S.; Brown, J.R.; Colman, R.A.; Delage, F.; Power, S.B.; Moise, A.F.; Zhang, H. Uncertainty in CMIP6 Climate Change Projections for the Australian Monsoon is tied to Hemispheric-Scale Changes. *Ess Open Arch.* **2019**, *47*, 1–23. [CrossRef]
53. Ongoma, V.; Chen, H.; Gao, C. Projected Changes in Mean Rainfall and Temperature over East Africa Based on CMIP5 Models. *Int. J. Climatol.* **2018**, *38*, 1375–1392. [CrossRef]
54. Dike, V.N.; Shimizu, M.H.; Diallo, M.; Lin, Z.; Nwofor, O.K.; Chineke, T.C. Modelling Present and Future African Climate using CMIP5 Scenarios in HadGEM2-ES. *Int. J. Climatol.* **2014**, *35*, 1784–1799. [CrossRef]
55. Mokhtar, M.A.E.; Laouane, R.B.; Anli, M.; Boutasknit, A.; Fakhech, A.; Wahbi, S.; Meddich, A. Climate Change and Its Impacts on Oases Ecosystem in Morocco. In *Advances in Environmental Engineering and Green Technologies*; IGI Global: Hershey, PA, USA, 2019.
56. Driouech, F.; Stafi, H.; Khouakhi, A.; Moutia, S.; Badi, W.; Elrhaz, K.; Chehbouni, A.G. Recent Observed Country-Wide Climate Trends in Morocco. *Int. J. Climatol.* **2020**, *41*, E855–E874. [CrossRef]
57. Brahim, Y.A.; Saidi, M.E.M.; Kouraiss, K.; Sifeddine, A.; Bouchaou, L. Analysis of Observed Climate Trends and High Resolution Scenarios for the 21st Century in Morocco. *J. Mater. Environ. Sci.* **2016**, *8*, 1375–1384.
58. Filahi, S.; Tramblay, Y.; Mouhir, L.; Diaconescu, E.P. Projected Changes in Temperature and Precipitation Indices in Morocco from High-Resolution Regional Climate Models. *Int. J. Climatol.* **2017**, *37*, 4846–4863. [CrossRef]
59. Bouramdane, A.A. Identifying Large-Scale Photovoltaic and Concentrated Solar Power Hot Spots: Multi-Criteria Decision-Making Framework. *Int. Conf. Energy Environ. Res. (ICEER 2023)* **2022**, *17*. [CrossRef]
60. Bouramdane, A.A. Site Suitability of Offshore Wind Energy: A Combination of Geographic Referenced Information and Analytic Hierarchy Process. *Int. Conf. Energy Environ. Res. (ICEER 2023)* **2022**, *17* . [CrossRef]
61. Bouramdane, A.A. Spatial Suitability Assessment of Onshore Wind Systems Using the Analytic Hierarchy Process. *Int. Conf. Energy Environ. Res.* **2022**. *17*. [CrossRef]
62. Nkrumah, F.; Quagraine, K.A.; Quagraine, K.T.; Wainwright, C.E.A.; Quenum, G.M.; Amankwah, A.; Klutse, N.A.B. Performance of CMIP6 HighResMIP on the Representation of Onset and Cessation of Seasonal Rainfall in Southern West Africa. *Atmosphere* **2022**, *13*, 999. [CrossRef]
63. Ayugi, B.O.; Dike, V.N.; Ngoma, H.; Babaousmail, H.; Mumo, R.; Ongoma, V. Future Changes in Precipitation Extremes over East Africa Based on CMIP6 Models. *Water* **2021**, *13*, 2358. [CrossRef]
64. Almazroui, M.; Saeed, F.; Saeed, S.; Islam, M.N.; Ismail, M.F.; Klutse, N.A.B.; Siddiqui, M.H. Projected Change in Temperature and Precipitation Over Africa from CMIP6. *Earth Syst. Environ.* **2020**, *4*, 455–475. [CrossRef]
65. Adam, S.; Reber, U.; Häussler, T.; Schmid-Petri, H. How Climate Change Skeptics (Try to) Spread their Ideas: Using Computational Methods to Assess the Resonance Among Skeptics' and Legacy Media. *PLoS ONE* **2020**, *15*, e0240089. [CrossRef]
66. Busch, T.; Judick, L. Climate Change—that is Not Real! A Comparative Analysis of Climate-Sceptic Think Tanks in the USA and Germany. *Clim. Chang.* **2021**, *164*, 1–23. [CrossRef]
67. Michler, J.D.; Baylis, K.; Arends-Kuenning, M.P.; Mazvimavi, K. Conservation Agriculture and Climate Resilience. *J. Environ. Econ. Manag.* **2019**, *93*, 148–169. [CrossRef] [PubMed]

68. Ma, B.; Hu, C.; Zhang, J.; Ulbricht, M.; Panglisch, S. Impact of Climate Change on Drinking Water Safety. *ACS ES T Water* **2022**, *2*, 259–261. [CrossRef]
69. Iturbide, M.; Gutiérrez, J.M.; Alves, L.M.; Bedia, J.; Cerezo-Mota, R.; Cimadevilla, E.; Cofiño, A.S.; Luca, A.D.; Faria, S.H.; Gorodetskaya, I.V.; et al. An Update of IPCC Climate Reference Regions for Subcontinental Analysis of Climate Model Data: Definition and Aggregated Datasets. *Earth Syst. Sci. Data* **2020**, *12*, 2959–2970. [CrossRef]
70. Global Wind Atlas. Available online: https://globalwindatlas.info/fr (accessed on 25 December 2022).
71. Moroccan Agency for Sustainable Energy (MASEN). Available online: https://solaratlas.masen.ma/map (accessed on 25 December 2022).
72. Ambrizzi, T.; Reboita, M.; da Rocha, R.P.; Llopart, M. The State of the Art and Fundamental Aspects of Regional Climate Modeling in South America. *Ann. N. Y. Acad. Sci.* **2019**, *1436*, 98–120. [CrossRef] [PubMed]
73. Climate Data Store (CDS) of the Copernicus Climate Change Service (C3S). Available online: https://cds.climate.copernicus.eu/ (accessed on 25 December 2022).
74. Riahi, K.; van Vuuren, D.; Kriegler, E.; Edmonds, J.; O'Neill, B.C.; Fujimori, S.; Bauer, N.; Calvin, K.V.; Dellink, R.; Fricko, O.; et al. The Shared Socioeconomic Pathways and their Energy, Land Use, and Greenhouse Gas Emissions Implications: An Overview. *Glob. Environ. Chang.-Hum. Policy Dimens.* **2017**, *42*, 153–168. [CrossRef]
75. van Vuuren, D.P.; Stehfest, E.; Gernaat, D.E.; Doelman, J.C.; van den Berg, M.; Harmsen, M.; de Boer, H.S.; Bouwman, L.; Daioglou, V.; Edelenbosch, O.Y.; et al. Energy, Land-Use and Greenhouse Gas Emissions Trajectories Under A Green Growth Paradigm. *Glob. Environ. Chang.-Hum. Policy Dimens.* **2017**, *42*, 237–250. [CrossRef]
76. Fricko, O.; Havlík, P.; Rogelj, J.; Klimont, Z.; Gusti, M.; Johnson, N.; Kolp, P.W.; Strubegger, M.; Valin, H.; Amann, M.; et al. The Marker Quantification of the Shared Socioeconomic Pathway 2: A Middle-of-the-Road Scenario for the 21st Century. *Glob. Environ. Chang.-Hum. Policy Dimens.* **2017**, *42*, 251–267. [CrossRef]
77. Fujimori, S.; Hasegawa, T.; Masui, T.; Takahashi, K.; Herran, D.S.; Dai, H.; Hijioka, Y.; Kainuma, M. SSP3: AIM Implementation of Shared Socioeconomic Pathways. *Glob. Environ. Chang.-Hum. Policy Dimens.* **2017**, *42*, 268–283. [CrossRef]
78. Calvin, K.V.; Bond-Lamberty, B.; Clarke, L.; Edmonds, J.A.; Eom, J.; Hartin, C.A.; Kim, S.H.; Kyle, P.; Link, R.; Moss, R.H.; et al. The SSP4: A World of Deepening Inequality. *Glob. Environ. Chang.-Hum. Policy Dimens.* **2017**, *42*, 284–296. [CrossRef]
79. Kriegler, E.; Bauer, N.; Popp, A.; Humpenöder, F.; Leimbach, M.; Strefler, J.; Baumstark, L.; Bodirsky, B.L.; Hilaire, J.; Klein, D.; et al. Fossil-Fueled Development (SSP5): An Energy and Resource Intensive Scenario for the 21st Century. *Glob. Environ. Chang.-Hum. Policy Dimens.* **2017**, *42*, 297–315. [CrossRef]
80. Rogelj, J.; Popp, A.; Calvin, K.V.; Luderer, G.; Emmerling, J.; Gernaat, D.E.; Fujimori, S.; Strefler, J.; Hasegawa, T.; Marangoni, G.; et al. Scenarios Towards Limiting Global Mean Temperature Increase Below 1.5 °C. *Nat. Clim. Chang.* **2018**, *8*, 325–332. [CrossRef]
81. Carbon Brief. Available online: https://www.carbonbrief.org/ (accessed on 25 December 2022).
82. ECMWF Confluence Wiki. CMIP6: Global Climate Projections. Available online: https://confluence.ecmwf.int/display/CKB/CMIP6%3A+Global+climate+projections#CMIP6:Globalclimateprojections-Models (accessed on 25 December 2022).
83. ES-DOC Interface. Available online: https://explore.es-doc.org/cmip6/models/ (accessed on 25 December 2022).
84. Ridley, J.K.; Menary, M.B.; Kuhlbrodt, T.; Andrews, M.B.; Andrews, T. MOHC HadGEM3-GC31-LL Model Output Prepared for CMIP6 CMIP. 2018. Available online: https://www.wdc-climate.de/ui/cmip6?input=CMIP6.CMIP.MOHC.HadGEM3-GC31-LL.historical (accessed on 25 December 2022).
85. Volodin, E.M.; Mortikov, E.V.; Kostrykin, S.V.; Galin, V.Y.; Lykossov, V.N.; Gritsun, A.; Diansky, N.A.; Gusev, A.V.; Iakovlev, N.; Shestakova, A.A.; et al. Simulation of the Modern Climate Using the INM-CM48 Climate Model. *Russ. J. Numer. Anal. Math. Model.* **2018**, *33*, 367–374. [CrossRef]
86. Volodin, E.M. Possible Climate Change in Russia in the 21st Century Based on the INM-CM5-0 Climate Model. *Russ. Meteorol. Hydrol.* **2022**, *47*, 327–333. [CrossRef]
87. Boucher, O.; Servonnat, J.; Albright, A.L.; Aumont, O.; Balkanski, Y.; Bastrikov, V.; Bekki, S.; Bonnet, R.; Bony, S.; Bopp, L.; et al. Presentation and Evaluation of the IPSL-CM6A-LR Climate Model. *J. Adv. Model. Earth Syst.* **2020**, *12*, e2019MS002010. [CrossRef]
88. Hajima, T.; Watanabe, M.; Yamamoto, A.; Tatebe, H.; Noguchi, M.A.; Abe, M.; Ohgaito, R.; Ito, A.; Yamazaki, D.; Okajima, H.; et al. Description of the MIROC-ES2L Earth System Model and Evaluation of its Climate—Biogeochemical Processes and Feedbacks. *Geosci. Model Dev. Discuss.* **2019**, *13*, 1–73. [CrossRef]
89. Mauritsen, T.; Bader, J.; Becker, T.; Behrens, J.; Bittner, M.; Brokopf, R.; Brovkin, V.A.; Claussen, M.; Crueger, T.; Esch, M.; et al. Developments in the MPI-M Earth System Model Version 1.2 (MPI-ESM1.2) and its Response to Increasing CO_2. *J. Adv. Model. Earth Syst.* **2019**, *11*, 998–1038. [CrossRef]
90. Sellar, A.A.; Jones, C.G.; Mulcahy, J.P.; Tang, Y.; Yool, A.; Wiltshire, A.; O'Connor, F.M.; Stringer, M.; Hill, R.; Palmiéri, J.; et al. UKESM1: Description and Evaluation of the U.K. Earth System Model. *J. Adv. Model. Earth Syst.* **2019**, *11*, 4513–4558. [CrossRef]
91. Giorgi, F.; Jones, C.; Asrar, G.R. Addressing Climate Information Needs At the Regional Level: The CORDEX Framework. *World Meteorol. Organ. (WMO) Bull.* **2009**, *58*, 175.
92. Wang, Y.; Leung, L.R.; McGregor, J.L.; Lee, D.; Wang, W.; Ding, Y.; Kimura, F. Regional Climate Modeling: Progress, Challenges, and Prospects. *J. Meteorol. Soc. Jpn.* **2004**, *82*, 1599–1628. [CrossRef]
93. Mearns, L.; Gutowski, W.J.; Jones, R.G.; Leung, R.; McGinnis, S.; Nunes, A.M.B.; Qian, Y. A Regional Climate Change Assessment Program for North America. *Eos, Trans. Am. Geophys. Union* **2009**, *90*, 311–311. [CrossRef]

94. Christensen, J.H.; Christensen, O.B. A Summary of the PRUDENCE Model Projections of Changes in European Climate By the End of this Century. *Clim. Chang.* **2007**, *81*, 7–30. [CrossRef]
95. van Meijgaard, E.; van Ulft, L.H.; Lenderink, G.; Roode, S.R.; Wipfler, E.; Boers, R.; Timmermans, R. *Refinement and Application of a Regional Atmospheric Model for Climate Scenario Calculations of Western Europe*; KVR: Rotterdam, The Netherlands, 2012.
96. JacobJuliane, D.; SamuelssonSamuel, P. *EURO-CORDEX: New High-Resolution Climate Change Projections for European Impact Research*; Regional Environmental Change; Springer: Berlin, Germany, 2013.
97. Med-CORDEX. Available online: https://www.medcordex.eu/ (accessed on 25 December 2022).
98. Suzuki, T. Seasonal Variation of the ITCZ and Its Characteristics Over Central Africa. *Theor. Appl. Climatol.* **2011**, *103*, 39–60. [CrossRef]
99. Knippertz, P.; Christoph, M.; Speth, P. Long-Term Precipitation Variability in Morocco and the Link to the Large-Scale Circulation in Recent and Future Climates. *Meteorol. Atmos. Phys.* **2003**, *83*, 67–88. [CrossRef]
100. Donat, M.G.; Peterson, T.C.; Brunet, M.; King, A.D.; Almazroui, M.; Kolli, R.K.; Boucherf, D.; Al-Mulla, A.Y.; Nour, A.Y.; Aly, A.A.; et al. Changes in Extreme Temperature and Precipitation in the Arab Region: Long-Term Trends and Variability Related to ENSO and NAO. *Int. J. Climatol.* **2014**, *34*, 581–592. [CrossRef]
101. Trenberth, K.E. Changes in Precipitation with Climate Change. *Clim. Res.* **2011**, *47*, 123–138. [CrossRef]
102. Ayugi, B.O.; Zhidong, J.; Zhu, H.; Ngoma, H.; Babaousmail, H.; Rizwan, K.; Dike, V.N. Comparison of CMIP6 and CMIP5 Models in Simulating Mean and Extreme Precipitation over East Africa. *Int. J. Climatol.* **2021**, *41*, 6474 –6496. [CrossRef]
103. Gidden, M.J.; Riahi, K.; Smith, S.J.; Fujimori, S.; Luderer, G.; Kriegler, E.; van Vuuren, D.P.; van den Berg, M.; Feng, L.; Klein, D.; et al. Global Emissions Pathways Under Different Socioeconomic Scenarios for Use in CMIP6: A Dataset of Harmonized Emissions Trajectories Through the End of the Century. *Geosci. Model Dev.* **2018**, *12*, 1443–1475. [CrossRef]
104. Lehner, F.; Deser, C.; Maher, N.; Marotzke, J.; Fischer, E.M.; Brunner, L.; Knutti, R.; Hawkins, E. Partitioning Climate Projection Uncertainty with Multiple Large Ensembles and CMIP5/6. *Earth Syst. Dyn.* **2020**, *11*, 491–508. [CrossRef]
105. Dosio, A.; Jury, M.W.; Almazroui, M.; Ashfaq, M.; Diallo, I.; Engelbrecht, F.; Klutse, N.A.B.; Lennard, C.J.; Pinto, I.; Sylla, M.B.; et al. Projected Future Daily Characteristics of African Precipitation Based on Global (CMIP5, CMIP6) and Regional (CORDEX, CORDEX-CORE) Climate Models. *Clim. Dyn.* **2021**, *57*, 3135–3158. [CrossRef]
106. Bouramdane, A.A. Transition Énergétique: Problématiques de Recherche. *énergies/mines carrières* **2022**, zenodo.7324462. [CrossRef]
107. Byrne, M.P.; O'Gorman, P.A. Link Between Land-Ocean Warming Contrast and Surface Relative Humidities in Simulations with Coupled Climate Models. *Geophys. Res. Lett.* **2013**, *40*, 5223–5227. [CrossRef]
108. Pepin, N.C.; Arnone, E.; Gobiet, A.; Haslinger, K.; Kotlarski, S.; Notarnicola, C.; Palazzi, E.; Seibert, P.; Serafin, S.; Schöner, W.; et al. Climate Changes and Their Elevational Patterns in the Mountains of the World. *Rev. Geophys.* **2022**, *60*, e2020RG000730. [CrossRef]
109. Yao, T.; Zhang, Q. Study on Land-Surface Albedo over Different Types of Underlying Surfaces in North China. *Acta Phys. Sin.* **2014**, *63*, .. [CrossRef]
110. Lhermitte, S.; Abermann, J.; Kinnard, C. Albedo Over Rough Snow and Ice Surfaces. *Cryosphere* **2014**, *8*, 1069–1086. [CrossRef]
111. Clem, K.R.; Fogt, R.L.; Turner, J.; Lintner, B.R.; Marshall, G.J.; Miller, J.R.; Renwick, J.A. Record Warming at the South Pole During the Past Three Decades. *Nat. Clim. Chang.* **2020**, *10*, 762–770. [CrossRef]
112. Hahn, L.C.; Armour, K.C.; Zelinka, M.D.; Bitz, C.M.; Donohoe, A. Contributions to Polar Amplification in CMIP5 and CMIP6 Models. *Front. Earth Sci.* **2021**, *9*, 710036. [CrossRef]
113. Walsh, J.E. Intensified Warming of the Arctic: Causes and Impacts on Middle Latitudes. *Glob. Planet. Chang.* **2014**, *117*, 52–63. [CrossRef]
114. Francis, J.A.; Skific, N. Evidence Linking Rapid Arctic Warming to Mid-Latitude Weather Patterns. *Philos. Trans. Ser. Math. Phys. Eng. Sci.* **2015**, *373*, 20140170. [CrossRef]
115. Alkama, R.; Taylor, P.C.; Martin, L.G.S.; Douville, H.; Duveiller, G.; Forzieri, G.; Swingedouw, D.; Cescatti, A. Clouds Damp the Radiative Impacts of Polar Sea Ice Loss. *Cryosphere* **2020**, *14*, 2673–2686. [CrossRef]
116. Koutsoyiannis, D. Clausius–Clapeyron Equation and Saturation Vapour Pressure: Simple Theory Reconciled with Practice. *Eur. J. Phys.* **2012**, *33*, 295–305. [CrossRef]